

# Skeletal distribution of bisphosphonate after elution from porous implants

Kimberly McKenzie, Department of Biomedical Engineering  
McGill University, Montreal, QC

October 2009

A thesis submitted to McGill University in partial fulfillment of the  
requirements of the degree of Master of Engineering

© Copyright Kimberly McKenzie 2009

## **ACKNOWLEDGEMENTS**

---

I would first like to thank my supervisor Dr. Dennis Bobyn for his unwavering support and guidance throughout this masters degree. He was always willing to help me in any way possible and was genuinely interested in enriching my learning experience at McGill. His enthusiasm for and depth of knowledge of orthopedics helped me get the most out of my time as a student.

I would also like to thank Dr. Michael Tanzer for implanting and retrieving the implants used in this study. In addition to his surgical skills, he provided valuable advice and support for the many aspects involved with this project, from experimental design to abstract submission for conferences.

Dorota Karabasz introduced me to the techniques and equipment I would need to use throughout my project and for this I am grateful. She was great company in the lab and I regret that we worked together for only a short time.

Dr. Dieter Reinhardt and Dr. Peter Roughley generously provided me with not only autoradiography film and cassettes, but also invaluable advice about the technique and what I might do to optimize the results. Their help with my project was greatly appreciated.

Kind donations from Novartis Pharma and Zimmer provided the <sup>14</sup>C-labelled zoledronic acid and tantalum implants used in this project.

## **ABSTRACT**

---

Skeletal attachment to an implant can be enhanced by locally delivering the bisphosphonate zoledronic acid from an implant. The purpose of this study was to map the skeletal distribution of locally delivered zoledronic acid.

A porous tantalum implant coated with hydroxyapatite and  $^{14}\text{C}$ -labelled zoledronic acid was implanted into the left femur of three dogs. After one year bone samples were taken from sites near to and distant from the implant. The amount of drug in each sample was determined using liquid scintillation counting and its distribution in peri-implant bone was additionally demonstrated using autoradiography.

All distant skeletal bone samples contained  $\leq 11.8$  ng/g zoledronic acid whereas bone immediately adjacent to the implant contained 388 ng/g. There was a 10-fold to 100-fold decrease in zoledronic acid content in bone just 1 or 2 cm away from the implant. Autoradiographs of thin bone-implant sections and bone sections revealed the highest concentration of zoledronic acid within and immediately adjacent to the implant. These data demonstrated for the first time that zoledronic acid eluted from an implant remained mainly local, with minimal systemic distribution.

## **RÉSUMÉ**

---

L'attachement squelettique à un implant peut être amélioré en apportant de l'acide zoledronique de bisphosphonate de façon locale depuis l'implant. Le but de la présente étude était d'évaluer la distribution squelettique de l'acide zoledronique localement généré.

Un implant poreux de tantale enduit d'hydroxyapatite et d'acide  $^{14}\text{C}$  zoledronique a été implanté dans le fémur gauche de trois chiens. Après un an, plusieurs échantillons d'os, proches et éloignés de l'implant, ont été prélevés. La quantité de médicament dans chaque échantillon a ensuite été déterminée en utilisant un comptage par scintillation liquide; la distribution dans l'os autour de l'implant a aussi été démontré par autoradiographie.

Tous les échantillons prélevés loin de l'implant contenaient  $\leq 11.8$  ng/g d'acide zoledronique alors que ceux prélevés immédiatement à côté de l'implant contenaient 388 ng/g. Une diminution de 10 à 100 fois dans la teneur en acide zoledronique a été notée dans l'os situé seulement à 1 ou 2 cm de l'implant. Les autoradiographies des sections minces d'os-implant et des sections d'os ont indiqué que la concentration la plus élevée en acide zoledronique se situait dans l'implant et immédiatement à côté. Ces données démontrent, pour la première fois, que l'acide zoledronique élué d'un implant reste principalement local, avec une distribution systémique minimale.

## **TABLE OF CONTENTS**

---

<b>1.0 INTRODUCTION.....</b>	<b>1</b>
1.1 Fixation.....	1
1.1.1 Bone cement.....	2
1.1.2 Biologic fixation.....	3
1.1.2.1 Textured surfaces.....	3
1.1.2.2 Calcium-phosphate coatings.....	5
1.1.2.3 Extracellular matrix materials.....	6
1.2 Impediments to effective, long-term fixation.....	7
1.2.1 Implant movement.....	7
1.2.2 Gaps between implant and bone.....	7
1.2.3 Loosening.....	8
1.2.4 Other challenges to achieving fixation.....	9
<b>2.0 LITERATURE REVIEW.....</b>	<b>10</b>
2.1 Bisphosphonates.....	10
2.1.1 Bisphosphonate structure.....	10
2.1.2 Bisphosphonate mechanism of action.....	11
2.2 Zoledronic acid.....	12
2.3 Systemically administered bisphosphonates.....	13
2.3.1 Disadvantages of systemically administered bisphosphonates.....	16
2.4 Locally delivered bisphosphonates.....	19
2.5 Locally delivered zoledronic acid.....	20
<b>3.0 PURPOSE.....</b>	<b>23</b>
<b>4.0 METHODS.....</b>	<b>24</b>
4.1 Preparation of tantalum implants.....	24
4.2 Surgical procedure.....	25
4.3 Procedure for liquid scintillation analysis.....	26
4.3.1 Tissue harvest.....	26
4.3.2 Defatting and dehydrating.....	29
4.3.3 Dissolving of specimens.....	30
4.3.4 Analysis of radioactivity in dissolved specimens.....	30
4.3.5 Analysis of radioactivity in implants.....	31
4.3.6 Analysis of radioactivity in defatting and dehydrating solutions.....	31
4.4 Autoradiography.....	32
<b>5.0 RESULTS.....</b>	<b>35</b>
5.1 Systemic distribution of zoledronic acid.....	35
5.2 Implants and implant-containing femora.....	39
5.3 Analysis of defatting and dehydrating solutions.....	49
5.4 Autoradiography.....	49

<b>6.0 DISCUSSION</b>	<b>55</b>
6.1 Distribution of zoledronic acid	55
6.2 Distribution at sub-therapeutic levels	59
6.3 Elution of zoledronic acid from coated implants	60
6.4 Optimizing drug elution	67
<b>7.0 CONCLUSION</b>	<b>69</b>
<b>8.0 REFERENCES</b>	<b>70</b>

## LIST OF FIGURES

<b>Figure 1.</b> Bone cement is prepared by the surgeon in the operating room at the time of surgery and is applied immediately into or onto bony sites of implantation	2
<b>Figure 2.</b> (A) Cross section of bone growth into the pores created by a fiber wire coating (struts appear black, void space is white). (B) Scanning electron micrograph of a fiber wire coating	4
<b>Figure 3.</b> Porous tantalum with its highly interconnected and uniformly shaped pores. This material has a porosity of about 75-80% and is used to fabricate implants in clinical use today	6
<b>Figure 4.</b> Basic bisphosphonate structure	11
<b>Figure 5.</b> Chemical structure of zoledronic acid	13
<b>Figure 6.</b> An implant held in a spindle jig as zoledronic acid is manually applied to the implant surface	25
<b>Figure 7.</b> Femora and other long bones were sliced into transverse serial sections approximately 1 cm thick	27
<b>Figure 8.</b> Contact radiographs of each implant-containing femur were taken to ensure the implant was cut into 6 roughly equal-sized pieces. The proximal and distal ends of implants in two of the dogs were embedded in acrylic and examined using autoradiography	27
<b>Figure 9.</b> As much bone as possible was removed from the outer surface of the implant. The amount of zoledronic acid in peri-implant bone - including what was scraped off the implant (lower left quadrant) - was determined separately from the amount on and within the implant	28
<b>Figure 10.</b> Samples from each dog were harvested in the same manner except with regard to implants. From Dog 1 and Dog 2 the proximal and distal ends of each implant including peri-implant bone were examined using autoradiography (section 4.4), while only the middle four segments were analysed using liquid scintillation spectrophotometry (section 4.3.4). From Dog 3 the entire implant and peri-implant bone was examined using liquid scintillation spectrophotometry only	29
<b>Figure 11.</b> Calibration curve used to calculate mass of zoledronic acid in tissue samples. The curve was generated using solutions of known zoledronic acid concentration. Image taken from Roberts, 2008	32
<b>Figure 12.</b> Implant-containing bone embedded in acrylic as it is being sectioned	34

<b>Figure 13.</b> Autoradiography cassette, and the opened cassette with slides arranged inside.....	34
<b>Figure 14.</b> Skeletal distribution of zoledronic acid (ng/g dry bone). Average zoledronic acid concentration in peri-implant bone was 388 ng/g dry bone.....	36
<b>Figure 15.</b> Zoledronic acid content (in ng) in each section of Dog 1's right femur. Note the greater masses in the metaphyses compared to the diaphysis.....	40
<b>Figure 16.</b> Zoledronic acid content (in ng) in each section of Dog 2's right femur. Note the greater masses in the metaphyses compared to the diaphysis.....	41
<b>Figure 17.</b> Zoledronic acid content (in ng) in each section of Dog 3's right femur. Note the greater masses in the metaphyses compared to the diaphysis.....	42
<b>Figure 18.</b> Zoledronic acid content (in ng) in femoral bone and implant in Dog 1. The mass of zoledronic acid in proximal and distal sections of the implant and surrounding bone could not be quantified since these segments were embedded in acrylic and sectioned for analysis by autoradiography.....	43
<b>Figure 19.</b> Zoledronic acid content (in ng) in femoral bone and implant in Dog 2. The mass of zoledronic acid in proximal and distal sections of the implant and surrounding bone could not be quantified since these segments were embedded in acrylic and sectioned for analysis by autoradiography. The implant appears to have deformed slightly upon insertion, but this would not have affected the results of this study.....	44
<b>Figure 20.</b> Zoledronic acid content (in ng) in femoral bone and implant in Dog 3. This was the only implant-containing femur for which the mass of zoledronic acid was quantified in all segments.....	45
<b>Figure 21.</b> Graph illustrating zoledronic acid concentration as a function of centimeter intervals along the femur. Note the peak peri-implant zoledronic acid concentration around the proximal half of the implant. Peri-implant bone possessed one to two orders of magnitude more zoledronic acid than bone slightly proximal or distal to the implant.....	49
<b>Figure 22.</b> Proximal serial sections of implant and surrounding bone from Dog 1 imaged in a contact radiograph (left) and a corresponding autoradiograph (right). The implant is present in the top three sections. The autoradiography reveals that zoledronic acid is strongly concentrated in and around the implant with diminished content distal to the implant and in surrounding bone.....	51
<b>Figure 23.</b> Distal serial sections of implant and surrounding bone from Dog 1 imaged in a contact radiograph (left) and a corresponding autoradiograph (right). The implant is present in the top five sections. The autoradiography reveals that zoledronic acid is strongly concentrated in and around the implant with diminished content distal to the implant and in surrounding bone. Zoledronic acid around the outer edge of the cortex is indicated by arrows.....	52

<b>Figure 24.</b> Proximal serial sections of implant and surrounding bone from Dog 2 imaged in a contact radiograph (left) and a corresponding autoradiograph (right). The implant is present in the top four sections. The autoradiography reveals that zoledronic acid is strongly concentrated in and around the implant with diminished content distal to the implant and in surrounding bone. Zoledronic acid around the outer edge of the cortex is indicated by arrows.....	53
<b>Figure 25.</b> Distal serial sections of implant and surrounding bone from Dog 2 imaged in a contact radiograph (left) and a corresponding autoradiograph (right). The implant is present in the top three sections. The autoradiography reveals that zoledronic acid is strongly concentrated in and around the implant with diminished content distal to the implant and in surrounding bone. Zoledronic acid around the outer edge of the cortex is indicated by arrows. The top section on the left appears incomplete because it was obliquely oriented within the embedding medium and was thus sectioned at an angle.....	54
<b>Figure 26.</b> Release rate of zoledronic acid from implants with or lacking a hydroxyapatite coating. Elution was done in water. All zoledronic acid was released from implants without a hydroxyapatite coating within 15 minutes. Note the initial burst release of zoledronic acid from hydroxyapatite-coated implants followed by a plateau out to 12 weeks. Image taken from Roberts, 2008.....	61
<b>Figure 27.</b> A porous tantalum implant plasma spray coated with hydroxyapatite is shown in A while a scanning electron micrograph of the surface is shown in B. Back-scattered scanning electron micrographs of cross-sections of the implant (C and D) show the distribution of plasma-sprayed hydroxyapatite on the implant surface. In C and D, tantalum struts appear white while hydroxyapatite appears grey. It is evident that plasma sprayed hydroxyapatite reaches only the outer surface of the implant's outer struts (indicated by white arrows).....	63

## LIST OF TABLES

<b>Table 1.</b> Average mass of zoledronic acid (in ng) per gram of tissue in all three dogs.....	37
<b>Table 2.</b> Mass of zoledronic acid (in ng) per gram of tissue in each of the three dogs. There are missing values because some tissues were not sampled. The mass of zoledronic acid found in each bone varied between dogs but in all samples, the mass of zoledronic acid was much less than in peri-implant bone.....	38
<b>Table 3.</b> Total mass of zoledronic acid (in µg) in right femora.....	39
<b>Table 4.</b> Mass of zoledronic acid on and within the implant, in peri-implant bone, and in the entire bone (excluding and including the implant). The mass of zoledronic acid in the left femurs of Dog 2 and Dog 1 could not be quantified since two segments from each femur were analyzed by autoradiography instead of liquid scintillation spectrophotometry.....	46
<b>Table 5.</b> Average mass of zoledronic acid per centimeter of implant.....	47



**Table 6.** Length of each implant segment analyzed using liquid  
scintillation spectrophotometry.....47

## **1.0 INTRODUCTION**

---

In 2006, nearly half a million Americans were discharged from hospitals after receiving a total or partial hip replacement surgery (1). About an equal number underwent knee replacement surgery. These numbers are expected to rise as today's aging population grows and the occurrence of joint degeneration grows with it. The usual cause of joint degeneration is some form of arthritis; in roughly 82% of patients who received a total hip replacement, osteoarthritis was the underlying diagnosis (2). Diagnoses in the remaining 18% comprised a variety of conditions such as rheumatoid arthritis or fracture. Although the long-term success rates treating such conditions with joint replacements are high, there are still a number of joint replacement design features that need to be refined.

### **1.1 Fixation**

In order for an implant to function properly it must be firmly attached to the skeleton. Without immediate and sufficient fixation an implant will be unable to restore joint function and the recipient will experience pain and decreased mobility. There are two main ways to achieve fixation of joint replacement implants - using bone cement or biologic fixation. Each is described below in greater detail.

### **1.1.1 Bone cement**

Since the 1960's a typical approach to achieving implant fixation was to use bone cement, a grout-like acrylic material prepared by the surgeon at the time of surgery and injected into or onto the bony sites of implantation (Figure 1). Once cured, the bone cement mechanically immobilizes the implant in situ. This fixation technique has been used successfully for decades and has very good long-term success rates (3-5), however, it has been supplanted to a large extent in recent years for various reasons (6). For example, if a cemented implant needs to be replaced at some point, removing the implant and surrounding bone cement may leave a patient with insufficient bone stock to adequately fix the replacement implant. Preparing the bone cement and waiting for it to cure provides another disadvantage as it requires extra time spent in the operating room. Bone cement also has somewhat limited mechanical properties and is prone to failure under exaggerated mechanical demands as typically occurs in younger, more active patients.



**Figure 1.** Bone cement is prepared by the surgeon in the operating room at the time of surgery and is applied immediately into or onto bony sites of implantation.

### ***1.1.2 Biologic fixation***

The other most common method for attaching implants to the skeleton involves some form of 'biologic fixation' in which the host bone heals to or forms directly on or within the implant surface. This requires careful surgical techniques and a very tight initial mechanical fit of the implant within bone (6). It also requires various design features such as textured, porous or calcium phosphate coatings that enable direct bonding with host bone through apposition or ingrowth. Extracellular matrix materials, though not yet in clinical use, are also being investigated for their potential ability to enhance bone formation.

#### ***1.1.2.1 Textured surfaces***

Implant surfaces may be textured using a variety of techniques. Beads or fiber wires may be sintered to the implant surface (Figure 2), an implant may be plasma sprayed with an appropriate material or cast with a specific surface topography, or microtexture may be created by grit-blasting. With porous implants, bone will grow into pores that have a diameter larger than 25  $\mu\text{m}$  - the minimum size required for osteon formation (7). Optimal speed and amount of ingrowth will occur within a pore size reported to be between approximately 100-500  $\mu\text{m}$  (8, 9). Most porous-coated implants in clinical use today use pore sizes within this range.

Another surface feature that affects implant fixation is surface topography. This parameter is often characterized by calculating the

average distance from the center line to the peaks and valleys over a given distance, a parameter designated  $R_a$ . Implants with microtextured surfaces possessing  $R_a$  values in the range of about 2 to 6  $\mu\text{m}$  have been shown to be conducive to direct bone apposition and the formation of improved mechanical stability (10-13).

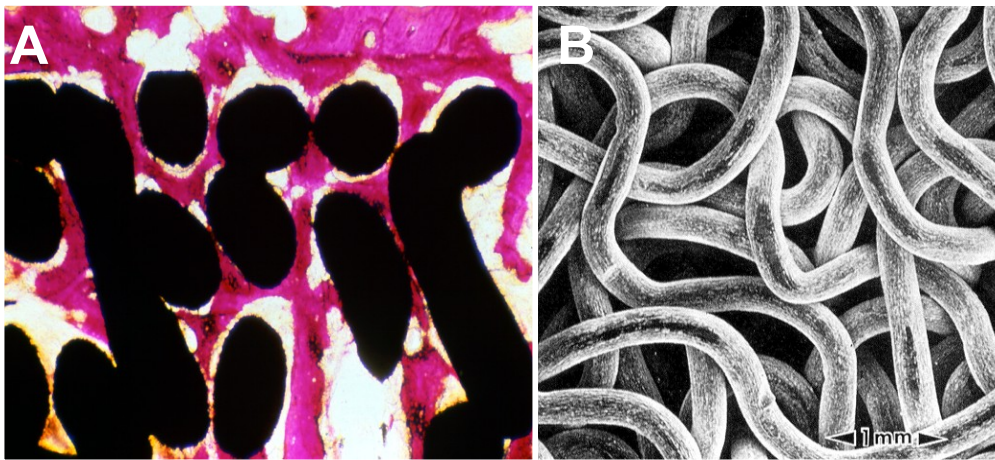


**Figure 2.** (A) Cross section of bone growth into the pores created by a fiber wire coating (struts appear black, void space is white). (B) Scanning electron micrograph of a fiber wire coating.

A material with a suitably textured and porous surface - and also the material used in this thesis - is porous tantalum. In vivo and in vitro, tantalum is highly corrosion resistant (14). As well, tantalum and its oxide have a low toxicity and elicit a benign host response. Porous tantalum has a few advantages over more traditional porous materials such as sintered beads or fiber wire coatings. In addition to having a microtextured surface (Figure 3), it has highly interconnected pores of fairly uniform geometry, a higher coefficient of friction against bone, and a lower bulk stiffness.

Porous tantalum can also be made with a higher porosity; sintered beads or fiber wire coatings have a volume porosity of about 30-50%, whereas that of porous tantalum is between 75-80% (15, 16). The higher porosity allows more and faster bone ingrowth, which leads to greater strength at the bone-implant interface and thus more stable fixation. Since 1997, porous tantalum has been used for a number of clinical purposes without necessitating a solid metal support structure. Some of these clinical uses include the fabrication of joint replacement components and spinal implants, or the treatment of avascular necrosis of the femoral head (16).

#### *1.1.2.2 Calcium-phosphate coatings*

For many years, calcium phosphate coatings such as tricalcium phosphate or hydroxyapatite have been applied to implant surfaces to improve osseointegration. Applying these coatings, which are similar in composition to natural bone, encourages effective fixation (17). Originally, the mechanism responsible for improved fixation was presumed to be chemical in nature (18). These “bioactive” coatings, as they have been called, were thought to provide Ca and P to bone forming around the implant. However, Hacking et al (19) found that the primary reason hydroxyapatite stimulated bone apposition was because of the microtextured surface that resulted after plasma spray deposition of the coating. Surface chemistry may still play a role in improving osseointegration, but that role appears to be much less significant than previously thought.

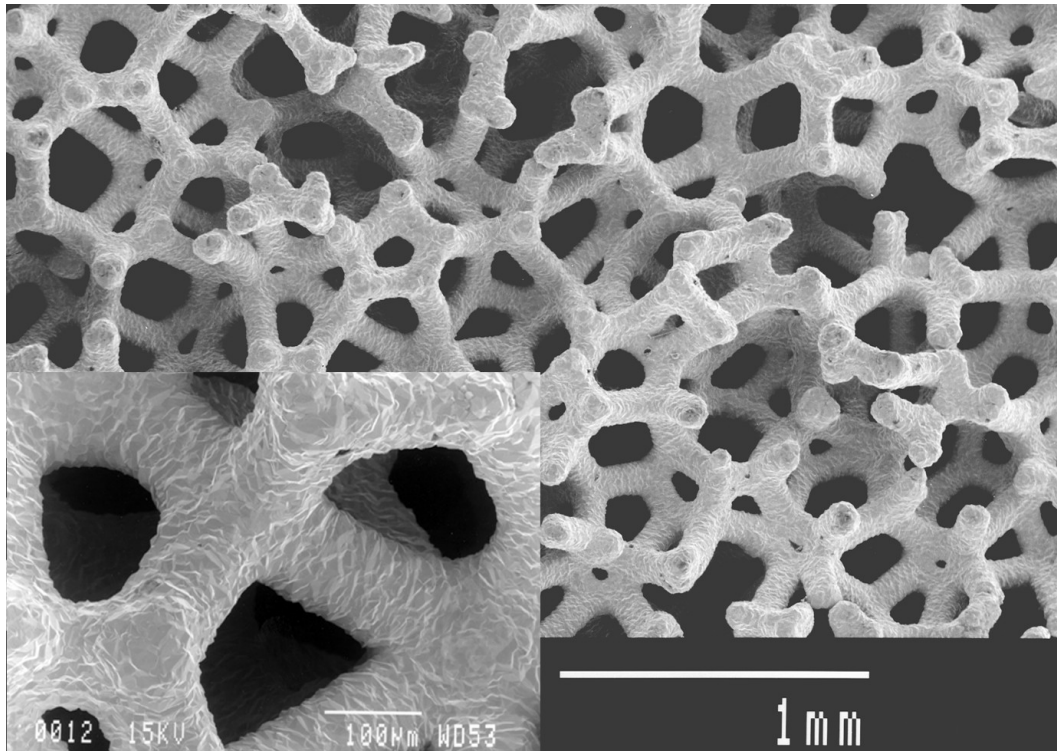


**Figure 3.** Porous tantalum with its highly interconnected and uniformly shaped pores. This material has a porosity of about 75-80% and is used to fabricate implants in clinical use today.

#### *1.1.2.3 Extracellular matrix materials*

Extracellular matrix components of bone are comprised of a variety of signaling molecules that regulate cellular activities like growth, differentiation, and apoptosis. While many of these components may contribute to the formation of new bone, a few in particular have been studied in animal models for their potential ability to augment implant fixation. Researchers have applied transforming growth factor- $\beta$ , bone morphogenetic proteins, collagen, and RGD (Arg-Gly-Asp) peptide to implant surfaces in an attempt to create a “bioactive” surface that promotes activities like osteoblast adhesion and proliferation (18, 20-23).

These approaches have met with varying degrees of success and considerable challenges remain; clinical application of these materials to enhance implant fixation is unlikely in the near future.

## ***1.2 Impediments to effective, long-term fixation***

### ***1.2.1 Implant movement***

Movement of the implant relative to surrounding bone immediately following surgery can hinder proper fixation. Bone ingrowth can occur with small displacements; about 28  $\mu\text{m}$  is tolerable as long as there is sufficient vascularity and no inflammatory response (21). However, larger displacements (of between 100-500  $\mu\text{m}$ ) can lead to the formation of woven bone, fibrous tissues, or, in extreme cases, a fibrous capsule (21, 24, 25). Because a fibrous interface is not as strong as a bony interface, this kind of implant attachment is less strong and is associated with a higher incidence of pain upon ambulation.

### ***1.2.2 Gaps between implant and bone***

To obtain sufficient bone ingrowth and fixation strength, contact between implant and bone must be as direct and continuous as possible (9). Gaps between bone and implant may occur due to anatomical irregularities in bone, an implant design ill-suited to the patient, or improper preparation and placement of the implant during surgery (26). Using bone cement is an effective way to fill gaps but in cases of cementless fixation care must be taken to minimize gaps. Hydroxyapatite



coating on an implant can enhance bone formation across a gap thereby improving fixation (27). However, there appears to be a limit to the size of a gap bone can traverse in sufficient quantities and at a satisfactory rate. Friedman et al (25) report that a space of as little as 2 mm may be enough to prevent bone from effectively bridging the gap between it and an implant. Dalton et al (28) found that it may be even smaller and that attachment strength and bone ingrowth are negatively affected by gaps of more than 1 mm.

### *1.2.3 Loosening*

Implant loosening is the main reason patients require revision surgery even if loosening does not clinically manifest itself until 10 years after joint replacement (29). Implant loosening may begin very soon after surgery and may be detected as a gradual implant migration (30). This gradual migration may be due to some combination of mechanical or biological causes such as obstructed circulation or physical damage sustained during surgery, fluid pressure, implant movement relative to surrounding bone, or gaps at the bone-implant interface (31-33). In any case, without immediate and sufficient fixation an implant will be unable to restore joint function and the recipient will experience pain and decreased mobility.

#### *1.2.4 Other challenges to achieving fixation*

Although current strategies to attain fixation are very effective, there are a number of situations in which fixation may be more difficult to achieve. In a patient who has just had a failed implant removed and needs a revision surgery there may not be enough bone stock remaining to adequately fix the device into place, or large gaps may exist between the implant and surrounding bone. Bone that is present may be of poor quality, as in patients who have bone metabolic disease like osteoporosis. Furthermore, patients may have a bone defect if they have undergone tumor resection or suffered trauma resulting in significant bone loss. To overcome these challenges, researchers have looked to pharmaceuticals to increase the amount and rate of peri-implant bone formation. Currently, the most promising compounds for this purpose are bisphosphonates.

## **2.0 LITERATURE REVIEW**

---

### **2.1 Bisphosphonates**

Bisphosphonates disrupt bone remodeling. In healthy individuals, bone is constantly being remodeled as osteoblasts lay down new bone mineral and osteoclasts resorb it. This is true in both normal intact bone as well as in bone that is healing. Since bisphosphonates have an affinity for solid-phase calcium, they accumulate in bone when administered systemically (34). As part of normal bone turnover, osteoclasts ingest bone mineral along with any bound bisphosphonate. Once inside the cell bisphosphonates interfere with osteoclast metabolism, reducing their effectiveness in bone resorption and triggering premature cell death (apoptosis). The reduction in osteoclastic activity ultimately tips the balance of bone turnover in favor of bone formation, the result being an increase in bone mass and density. The direct route into the osteoclast interior means that the drug will preferentially interfere with osteoclast metabolism as opposed to the metabolism of other cell types (35). Bisphosphonates are currently used worldwide in millions of patients for the treatment of osteoporosis.

#### ***2.1.1 Bisphosphonate structure***

The basic structure of bisphosphonates can be seen in Figure 4. In general, drugs of this class consist of two phosphonate groups bound to a central carbon atom. The phosphonate groups are responsible for the

affinity for calcium, although not all bisphosphonates have the same binding affinity (35). Also attached to the central carbon atom are two sidechains. The  $R_1$  position is usually occupied by a hydroxyl group - this enhances the bisphosphonate's affinity for calcium. The  $R_2$  group is more variable but determines potency. Generally, if the  $R_2$  group does *not* contain nitrogen, it is less potent; if the  $R_2$  group *does* contain nitrogen, it is more potent.

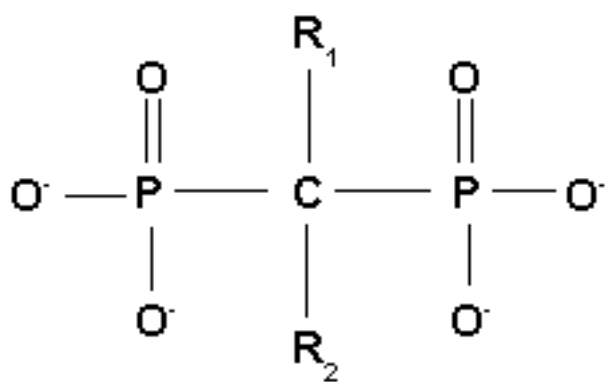


**Figure 4.** Basic bisphosphonate structure.

### 2.1.2 Bisphosphonate mechanism of action

Bisphosphonates that lack nitrogen inhibit bone resorption by interfering with pathways that are dependent on adenosine triphosphate (ATP) - a molecule comprised of inorganic pyrophosphate that is involved in various metabolic processes. When bisphosphonates are present in the cell, they become incorporated into ATP-analogues because they resemble inorganic pyrophosphates (34). Unlike inorganic pyrophosphates, however, the carbon of bisphosphonates is non-hydrolyzable meaning ATP-dependent pathways cannot proceed as

needed. Without these pathways an osteoclast cannot function and ultimately will undergo apoptosis.

Bisphosphonates that contain nitrogen inhibit osteoclast function by disrupting the mevalonate pathway (34). Under normal circumstances this pathway results in the production of isoprenoid lipids and sterols such as cholesterol, and is regulated in part by the enzyme farnesyl pyrophosphate synthase. By binding to and inhibiting the action of farnesyl pyrophosphate synthase, bisphosphonates inhibit post-translational modification of proteins (like Rab, Rac, and Rho) that help regulate osteoclast features such as the ruffled border. Without these features osteoclasts cannot resorb bone and effectively become dysfunctional.

## **2.2 Zoledronic acid**

The bisphosphonate that is the most potent inhibitor of osteoclast function is zoledronic acid (Figure 5). It is currently used in patients with certain types of cancer or cancer-related skeletal disorders such as multiple myeloma, hypercalcemia of malignancy, or bone metastases of solid tumors. It is also used in patients with bone metabolic disorders like Paget's disease, or osteoporosis - the most common diagnosis underlying zoledronic acid therapy. Studies have indicated that zoledronic acid can decrease the likelihood of fracture in patients with osteoporosis (36), and in patients who have had surgical repair of a hip fracture (37).

Patients typically receive zoledronic acid as an infusion given over 15 minutes with the number of dosages depending on the condition being

treated. For example, cancer patients receive 4 mg every 3-4 weeks whereas sufferers of osteoporosis receive 5 mg once a year.

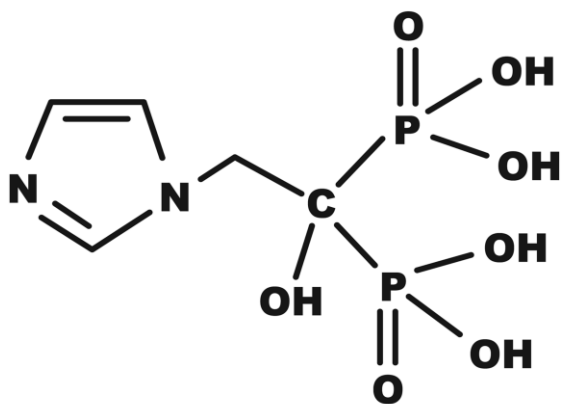


**Figure 5.** Chemical structure of zoledronic acid.

### 2.3 Systemically administered bisphosphonates

Although bisphosphonates are not yet approved by regulatory agencies for the purpose of enhancing peri-implant bone formation, a number of clinical trials have shown that systemically administered bisphosphonates can reduce bone resorption surrounding an implant. Arabmotlagh et al (38) administered alendronate to patients following total hip arthroplasty. They reported that administering alendronate six months postoperatively prevented early peri-prosthetic bone loss. Venesmaa et al (39) also administered alendronate to recipients of total hip replacements. These patients were treated for six months and compared to an appropriate control group. After the six month period there was significantly less peri-implant bone loss in the alendronate group.

In a longer-term alendronate study, Arabmotlagh et al (40) studied total hip replacement patients at one and six years postoperatively. Patients in this study had been given oral alendronate therapy for up to 10 weeks following surgery and experienced significantly reduced peri-prosthetic bone loss after one year. The antiresorptive effect of the alendronate therapy persisted six years after surgery.

Åstrand and Aspenberg (32) gave rats subcutaneous injections of clodronate, alendronate, or saline to observe the effects of bisphosphonate treatment with motion at a bone-metal interface. Titanium plates were screwed onto proximal rat tibiae and a depression was made in the middle of the plate. The portion of this depression contacting underlying bone formed the test surface. The researchers waited one week before beginning bisphosphonate treatment, and four weeks after implanting the plates before moving the implant. The implant was moved twice a day for two weeks, after which time tissues were examined histologically. Bone resorption around the implants was reduced, but only when very high doses of bisphosphonates were given. Although bisphosphonates in this study led to beneficial effects, the human doses equivalent to the ones used in this rat model would have been high enough to elicit side effects. The authors suggest that local delivery would be best to both improve fixation and avoid side effects.

Hilding et al (41) gave clodronate orally to patients for three weeks before and for 6 months after they received knee replacements. Radiostereometry indicated that migration of the prosthesis was reduced

during the first post-operative year and even after four years (33). They concluded that oral clodronate treatment can reduce the risk of implant loosening. They suggested that this likely occurs by inhibiting osteoclast activity and preventing post-operative peri-implant bone resorption.

Pamidronate is another bisphosphonate that has shown promising results in some clinical trials. Wilkinson et al (42) gave patients a single infusion of pamidronate after total hip arthroplasty. Six months after surgery study participants in the pamidronate group experienced significantly less bone loss (measured by changes in bone mineral density) compared to participants in the placebo group. The authors suggested their results warranted larger-scale, longer-term studies. A longer-term pamidronate study was performed by Shetty et al (43), who gave patients a single dose of pamidronate following total hip arthroplasty and assessed them five years after surgery. Contrary to expectations, however, Harris hip scores and radiological outcomes suggested that pamidronate given as a single postoperative dose does not affect clinical outcomes, nor did it protect against osteolytic lesions.

Though a variety of bisphosphonates have been systemically administered to joint replacement patients in clinical trials, zoledronic acid has not yet been studied in this context in humans. It has, however, been given intravenously in animal studies examining the fixation of porous tantalum implants (44). Bobyn et al reported significantly more bone ingrowth in dogs that received a zoledronic acid injection compared to control dogs. Although the authors were careful not to draw definitive



conclusions about their results, their study indicated that further investigation of such a therapy may be worthwhile.

### *2.3.1 Disadvantages of systemically administered bisphosphonates*

Unfortunately, systemically administering zoledronic acid, or any bisphosphonate for that matter, means it will be distributed throughout the body and this could cause side effects. Some of these side effects may be mild, such as the acute response (consisting of flu-like symptoms) that occurs after initial administration. The acute response occurs less frequently and with less severity after subsequent infusions. Of greater concern is the potential for patients with impaired renal function to develop renal toxicity. Osteonecrosis of the jaw has also been noted in a limited number of multiple myeloma patients receiving zoledronic acid who have also had dental procedures. More recently, the United States Food and Drug Administration issued a warning that some patients were developing severe and sometimes incapacitating musculoskeletal pain separate from the acute response (45). Most cases subsided when zoledronic acid therapy was discontinued.

Some researchers have suggested that systemic distribution of zoledronic acid may also be undesirable because of the long-term and potentially detrimental effects the drug may have on skeletal remodeling. Healthy remodeling leads to repair of the microdamage that occurs under conditions of normal, voluntary loading of the skeleton (46). If left unrepaired, perhaps due to oversuppression of osteoclast activity by

bisphosphonates, this microdamage may accumulate and possibly lead to fractures. Mashiba et al (47, 48) found a correlation between high doses of bisphosphonates and microdamage accumulation in the ribs of dogs who were given alendronate or risedronate. Allen et al (49) found that microdamage accumulated in the vertebrae of dogs who received clinical doses of alendronate or risedronate for one year. However, they reported no significant impairment of mechanical properties - an effect they attributed to increases in bone volume and mineralization. Chapurlat et al (50) examined the iliac crest of postmenopausal osteoporotic women who had received bisphosphonate treatment for an average of 6.5 years (minimum three years). The frequency of microdamage in bisphosphonate-treated women was not greater than in controls and the damage that was present appeared not to be related to age, length of bisphosphonate treatment, or extent of osteoclast suppression. The rigor of this study, however, has been called into question (51).

Zoledronic acid in particular has been studied for its effects on bone quality. Amanat et al (52) sampled femoral fracture sites in rats to determine hardness and elastic modulus. The animals had undergone closed fracture healing for 6 weeks and had intravenously received either saline or zoledronic acid. The authors reported that a single intravenous dose of zoledronic acid did not affect the intrinsic material properties of callus bone tissue. However, another study on the quality of zoledronic acid-treated bone reported slightly different results (53). In this study, zoledronic acid-coated implants were placed into the femoral canal of

dogs. After one year, nanoindentation tests indicated that peri-implant trabecular bone was harder and had a higher modulus than control bone. Experimental design and techniques used in each of the studies differed sufficiently that it is difficult to draw direct comparisons between the two. More work is needed to evaluate what effect zoledronic acid has on bone properties and what relevance this has on clinical applications.

Recently a number of authors have described clinical outcomes of patients who have received bisphosphonates other than zoledronic acid over the long term. These reports primarily concerned postmenopausal women taking alendronate who had suffered unusual fractures in the subtrochanteric region of the femur (54-56). The authors of these studies suggested that the fractures may be caused by accumulated microdamage or suppressed remodeling. Lee and Seibel (57) argued that these types of fractures are not exclusive to patients receiving bisphosphonates and may indicate nonadherence or poor patient health rather than a shortcoming of bisphosphonate therapy. Goh et al (54) also pointed out that many of the patients were given bisphosphonates because they were already at a higher risk of osteoporotic fractures. Although no definitive conclusions can be drawn about the link between long-term bisphosphonate use and clinically significant adverse skeletal effects, there is enough evidence to warrant further investigation.

Finally, systemically administering zoledronic acid may not be ideal because it is rapidly excreted once it reaches the circulatory system (34, 35, 58, 59). Once a patient has received an intravenous dose of zoledronic

acid, up to 55% of it is lost through the urine within 24 hours. Up to 90% is lost 48 hours after administration. Since the cost of zoledronic acid is quite high, the need to develop a more efficacious bisphosphonate delivery system is justified.

## **2.4 Locally delivered bisphosphonates**

To avoid the problems associated with systemically administering bisphosphonates, a number of studies have examined the effects of locally applied bisphosphonates. Using a gap model, Garbuz et al. (60) placed porous tantalum implants coated with calcium phosphate and alendronate into rabbit femurs for four weeks. Filling of the bone-implant gap as well as bone ingrowth were improved around the alendronate-coated implants. Garbuz and his group suggested delivering alendronate as an implant surface coating to encourage any bone defects to heal, and to improve success rates of revision joint replacement when a significant amount of bone has been lost.

Jakobsen et al (61) inserted porous-coated titanium implants with bone compaction into dog tibiae. They injected alendronate into the bone cavity prior to bone compaction and immediately before implant insertion, and examined the effects after 12 weeks. When alendronate was injected, implant fixation, bone-implant contact, and peri-implant bone volume fraction were significantly increased. Their findings indicated that local alendronate administration can enhance early implant osseointegration of implants inserted using bone compaction.

In 2009, Jakobsen et al (62) published a similar study, this time using hydroxyapatite-coated porous titanium implants. After 12 weeks, they found that alendronate treatment improved biomechanical fixation and increased the amount of peri-implant woven and lamellar bone. Alendronate did not, however, increase the amount of contact between bone and the hydroxyapatite coating.

Local bisphosphonate delivery studies have not been limited to animal models. Hilding and Aspenberg (33) conducted a study of 50 patients receiving cemented total knee replacements. Ibandronate or saline was applied to the tibial bone surface 1 minute before cement was applied and implant migration was monitored for up to 2 years after surgery using radiostereometry. Compared to saline controls, implants migrated significantly less when placed onto ibandronate-treated tibial plateaus. The authors reported that local pharmacological treatment can affect osteoclast activity and the mechanics of joint arthroplasty in a way that improves implant fixation.

## **2.5 Locally delivered zoledronic acid**

A number of studies have used animal models to investigate the effects of zoledronic acid elution from drug-coated implants. Tanzer et al (63) were the first to demonstrate that local elution of zoledronic acid enhances bone formation around and within porous orthopaedic implants. In this study porous tantalum rods were plasma spray coated with hydroxyapatite and then manually coated with zoledronic acid before

being placed into canine ulnae. Backscattered scanning electron microscopy and contact radiography of transverse sections of the implant-containing ulnae revealed that there was an average of 2.3 times more peri-implant bone around zoledronic acid-coated implants compared to the control group.

Gao et al (64) used ovariectomized rats to study the effects of solid titanium orthopaedic implants coated with hydroxyapatite and one of three bisphosphonates: ibandronate, pamidronate, or zoledronic acid. All three of the bisphosphonates enhanced bone formation and bone-implant integration after three months, with zoledronic acid eliciting the most pronounced effects.

Peter et al (65, 66) coated titanium cylinders with hydroxyapatite and zoledronic acid and implanted them into the femoral condyles of both normal (65) and ovariectomized rats (66). After three weeks the authors noted a window of zoledronic acid doses in which beneficial effects were seen. These effects included increased bone volume fraction, and improved mechanical stability as indicated by pull-out tests.

Increased bone formation has also been reported by Stadelmann et al (67), who implanted hydroxyapatite and zoledronic acid-coated rods into osteoporotic sheep femora. After four weeks, bone surface fraction increased by 50% in animals that received zoledronic acid. Bone surface fraction in the experimental group was significantly greater than in controls up to a distance of 400  $\mu\text{m}$  away from the outer layer of the implant.

Stadelmann et al (67), as well as Gao et al (64), and Peter et al (65), all

used animal models meant to mimic patients with osteoporotic bone. The beneficial effects reported in their studies indicate the potential usefulness of zoledronic acid-coated implants treating hip replacement patients who are also suffering from osteoporosis.

### **3.0 PURPOSE**

---

While many studies have shown that local elution of a bisphosphonate results in improved peri-implant bone formation and increased mechanical stability of the implant, it has not yet been determined how much drug that elutes from an implant remains local or is systemically distributed. If the drug remained primarily local the chance of side effects would be minimized as would skeletal exposure and the possibility of adverse long-term bone remodeling. This type of therapy would be well-suited to revision surgeries, when achieving initial fixation is particularly difficult and more peri-implant bone formation than usual is necessary. The present study was undertaken as an initial step towards developing drug-eluting implants. As such, the purpose of this study was to map the local and skeletal distribution of locally delivered zoledronic acid.



## 4.0 METHODS

---

### 4.1 Preparation of tantalum implants

Three porous tantalum (Trabecular Metal™) implants each measuring 50 mm long and 5 mm in diameter were obtained from Zimmer (Warsaw, IN). They had an average pore size of 430 µm and a volume porosity of approximately 75%. Implants were plasma spray coated with a 10-15 µm layer of hydroxyapatite (98% purity, 99% density, 64% crystallinity, calcium:phosphate ratio of 1.67). Each implant was placed into a spindle jig (Figure 6) and evenly coated with a solution of <sup>14</sup>C-labelled zoledronic acid. To prepare this solution, 100 µg of <sup>14</sup>C-labelled zoledronic acid (Novartis Pharma, Basel, Switzerland); specific activity 6.51 MBq/mg) was added to 500 µL of distilled deionized water. This dose was meant to be low enough to avoid toxicity to the animal, but high enough to be detectable. The zoledronic acid solution was thoroughly mixed before it was applied to the implant surface. A micropipette was used to apply 100 µL of the solution for each 1/5 rotation of the jig, drop by drop, such that the surface of the implant was saturated and evenly covered with the solution. Once the zoledronic acid solution had been applied, the implant was placed in a 50°C oven to dry overnight, then sterilized with ethylene oxide and packaged until the time of implantation.

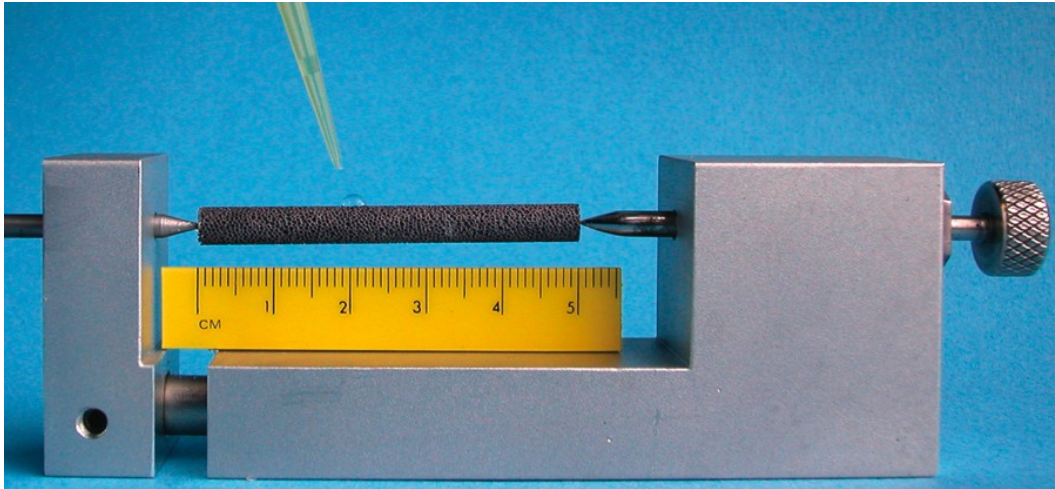


**Figure 6.** An implant held in a spindle jig as zoledronic acid is manually applied to the implant surface.

#### **4.2 Surgical procedure**

Three mongrel dogs between 2 and 5 years of age and weighing between 25 kg and 30 kg were used for this study. Each of the dogs received one implant in the left femoral intramedullary canal. Dogs were administered 0.05 cc/kg BAA 15 minutes prior to induction. Animals were induced using a 25 mg/kg dose of sodium pentobarbital and the hindlegs and mid-thoracic region were shaved. A 100 mg Fentanyl patch was placed on the mid-thoracic region. Anaesthesia was maintained with 3% Isoflurane and 2 L of oxygen. A total of 1 g of cefazolin was delivered: 5 cc prior to surgery and 5 cc after surgery.

Implants were put in place using standard sterile surgical techniques. An incision in the skin was made over the proximal end of the left femur. The gluteus medius was split and a hole (9 mm diameter) was drilled into the intramedullary canal of the femur through the piriformis

fossa. The implant was placed in the prepared hole and then tapped down the intramedullary canal until it was seated 10 mm below the level of the femoral neck. The drill site was then occluded with bone wax to avoid any radioactive drug eluting into the surrounding blood and escaping into the surrounding tissues. The wounds were then irrigated and closed in layers using resorbable Vicryl sutures. After extubation the dogs were given 0.01-0.02 mg/kg buprenorphine every 6-8 hours for approximately one day after surgery. Apo-cephalex antibiotic was administered (25-50mg/kg/day) following surgery. Dogs returned to normal weight-bearing activities one to two days after the operation.

### **4.3 Procedure for liquid scintillation analysis**

#### ***4.3.1 Tissue harvest***

After 12 months the animals were sacrificed and both soft and hard tissue samples were harvested from various sites. This included boney samples from both the left and right sides of the iliac crest, patella, clavicle, acetabulum, talus, scaphoid, metatarsals, glenoid fossa, metacarpals, ulna, radius, tibia, humerus, and femur of both the right and left extremities, as well as small pieces of liver, kidney, heart, spleen, lung and the left and right vastus lateralis. Once excised, tissues were frozen until needed. Long bones were serially sectioned (Figure 7) using a bandsaw (blade thickness of 0.5 mm) and soft tissues were removed from bones before the bones were processed. Because sections were not precisely measured before cutting, the sections of each long bone do not

necessarily correspond to the sections of the contralateral bone, or to the sections of the same long bone in the other dogs.

Femora containing an implant were imaged by contact radiography in a Faxitron MX-20 (Hewlett-Packard) before being serially sectioned. Imaging was done to ensure that each implant was cut into six roughly equal-sized segments (Figure 8).



**Figure 7.** Femora and other long bones were sliced into transverse serial sections approximately 1 cm thick.

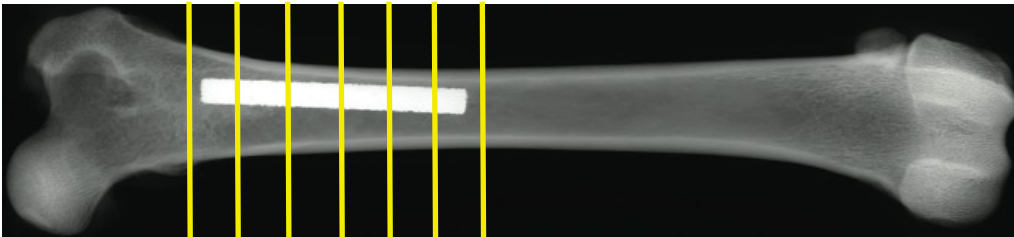


**Figure 8.** Contact radiographs of each implant-containing femur were taken to ensure the implant was cut into 6 roughly equal-sized pieces. The proximal and distal ends of implants in two of the dogs were embedded in acrylic and examined using autoradiography.

In two of the three implant-containing femora, two segments from each femur were reserved: one from the proximal end of each implant and one from the distal end. The preparation of these segments differed from the preparation of samples for liquid scintillation analysis and is described

below. For the remaining implant-containing segments (i.e., the segments not embedded in acrylic) in these two femora the bone surrounding each segment of implant was removed by dividing the cortex using a high speed Dremel tool and separating the cortical segments from the contained implant (Figure 9). Bone that adhered to the implant surface was manually scraped off with a scalpel and added to the cortical segments. This bone was removed so that radiation levels could be measured in the peri-implant bone as well as on and within the implant (Figure 10).

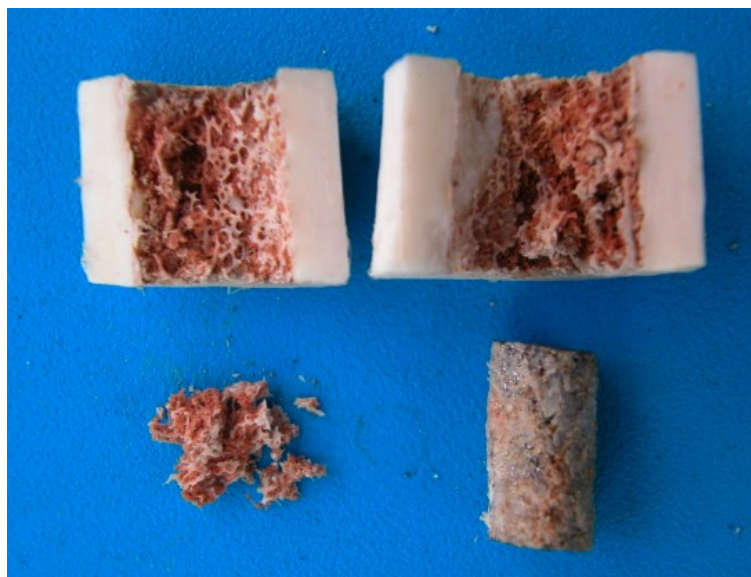


**Figure 9.** As much bone as possible was removed from the outer surface of the implant. The amount of zoledronic acid in peri-implant bone - including what was scraped off the implant (lower left quadrant) - was determined separately from the amount on and within the implant.

Radiation in the other bones and in soft tissues was measured for only a piece of each bone or soft tissue and not the entire bone or tissue. For example, only a piece of heart was sampled and not the entire organ. Thus the amount of drug in these samples can only be reported as a mass

of zoledronic acid per gram of tissue; the absolute mass of drug in each organ, tissue, or skeletal structure was not ascertained.

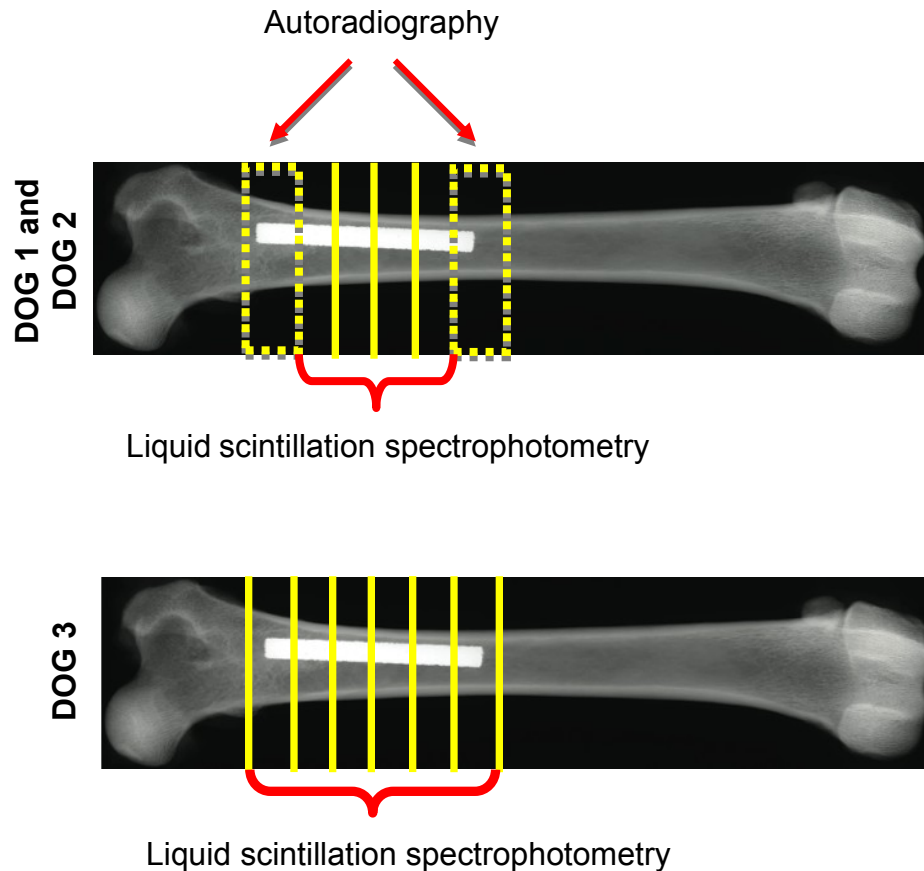


**Figure 10.** Samples from each dog were harvested in the same manner except with regard to implants. From Dog 1 and Dog 2 the proximal and distal ends of each implant including peri-implant bone were examined using autoradiography (section 4.4), while only the middle four segments were analysed using liquid scintillation spectrophotometry (section 4.3.4). From Dog 3 the entire implant and peri-implant bone was examined using liquid scintillation spectrophotometry only.

#### 4.3.2 Defatting and dehydrating

Tissue samples were first defatted in a solution of ether-acetone (1:1) for 24 hours. Enough ether-acetone was added to completely immerse the tissue. Samples were then fully immersed in 100% ethyl

alcohol for dehydration for 24 hours. After tissues were defatted and dehydrated they were placed in an oven at 42°C to dry overnight.

#### *4.3.3 Dissolving of specimens*

Once samples were dried they were transferred into pre-weighed vials. The vials and their contents were then weighed together to determine the dry mass of the sample.

In order to dissolve the tissues 6 N HCl was added to each vial in a ratio of approximately 25 mL of acid per 1 g of tissue. The amount of acid added was recorded for each sample. Once immersed in acid, samples were left in an oven at 42°C for one week and mixed occasionally using a Barnstead Type 16700 mixer.

#### *4.3.4 Analysis of radioactivity in dissolved specimens*

Once the tissue was dissolved, 600 µL of the dissolved tissue solution was added to a clean vial for analysis using liquid scintillation spectrophotometry. Solutions were diluted to 2 N HCl by adding 1.2 mL of distilled, deionized water to each vial. Liquid scintillation cocktail (Ultima Gold AB, Perkin Elmer USA) was added to each vial in a ratio of 10:1 cocktail to tissue solution. Thus, each 0.6 mL aliquot of dissolved tissue-HCl solution was diluted to a total volume of 19.8 mL. After mixing, <sup>14</sup>C levels were determined using a Packard Tri-Carb 2100TR liquid scintillator spectrometer. Measurements were recorded in counts per minute (CPM). Once background counts were subtracted the mass of zoledronic acid in

each vial could be ascertained using a 12-point calibration curve (Figure 11). Using the known masses of tissue and volumes of acid combined to form solutions for analysis, the liquid scintillation measurements were used to determine the concentration of zoledronic acid per gram of dry tissue for each sample.

#### *4.3.5 Analysis of radioactivity in implants*

Implants were subjected to the same defatting and drying procedures as described above. Dissolution and liquid scintillation procedures were also similar except that implant segments were removed from acid solutions once the encasing tissue and hydroxyapatite were dissolved. Also, implant segments were weighed before and after immersion in acid to determine the mass of material dissolved from the implant.

#### *4.3.6 Analysis of radioactivity in defatting and dehydrating solutions*

Ether-acetone and alcohol solutions were also analyzed using liquid scintillation spectrophotometry to determine if any drug was lost during defatting and dehydrating of specimens. Ether-acetone solutions from each sample were combined and analyzed together. The same was done with alcohol solutions. To test the combined solutions, 0.6 mL of each solution was placed into a vial containing liquid scintillation cocktail in a ratio of 3:1 cocktail to solution and analyzed with the liquid scintillation spectrophotometer.



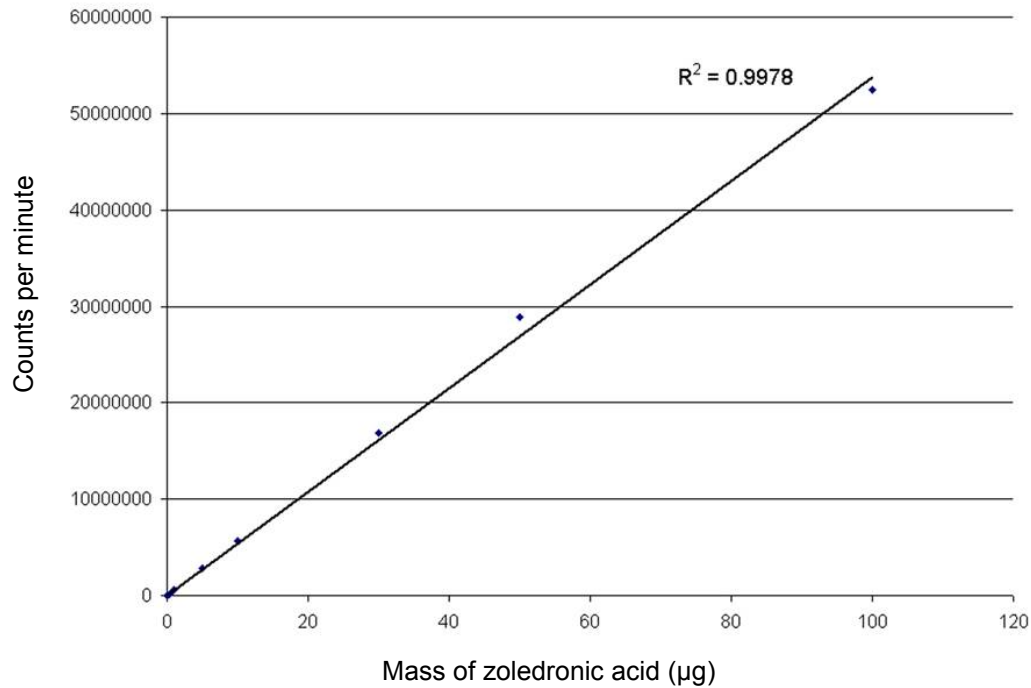


**Figure 11.** Calibration curve used to calculate mass of zoledronic acid in tissue samples. The curve was generated using solutions of known zoledronic acid concentration. Image taken from Roberts (68).

#### 4.4 Autoradiography

As mentioned previously, the proximal and distal bone-implant segments from two femora were reserved for alternate examination. This involved embedding in acrylic for undecalcified thin sectioning. First, bone segments were dehydrated in graded ethanol solutions of 70% and 95%. Segments were then placed in a 1:1 solution of ether-acetone for defatting, followed by a final alcohol solution of 100%. Segments were left in each solution for 24 hours. After drying overnight in an oven, bone segments were immersed in methylmethacrylate monomer (Sigma-Aldrich) with 0.05% benzoyl peroxide (Anachemia Science) in a hot water

bath and left to polymerize for 8-12 hours. After removal from the water bath, segments and partially polymerized monomer were cycled in a vacuum desiccator until degassing and infiltration was achieved, which took approximately 4-5 hours. Embedded segments were then left to cure at room temperature until they were hard - about five to seven days. Once hard, the embedded segments were sliced (Figure 12) into transverse serial sections about 0.5 mm in thickness. Contact radiographs of serial sections were taken according to the methods described above. Sections were then placed onto autoradiography film (Bioflex MSI film) in a dark room and sealed in a light-tight cassette for two weeks (Figure 13). The film was removed and developed in the dark room after two weeks of exposure to the sections.



**Figure 12.** Implant-containing bone embedded in acrylic as it is being sectioned.



**Figure 13.** Autoradiography cassette, and the opened cassette with slides arranged inside.

## **RESULTS**

---

### **5.1 Systemic distribution of zoledronic acid**

Figure 14 and Table 1 show the average mass of zoledronic acid per gram of tissue in all three dogs. The mass per gram of tissue in each tissue sample from all of the three dogs is shown in Table 2. No zoledronic acid was detected in any of the soft tissues. The concentration of zoledronic acid in osseous tissues (excluding the left femur) ranged from 1.9 ng/g bone to 7.1 ng/g. In long bones (excluding femora containing an implant), greater concentrations of zoledronic acid were found in the metaphyses as compared to the diaphyses. In peri-implant bone the average concentration was 377.2 ng/g of bone.

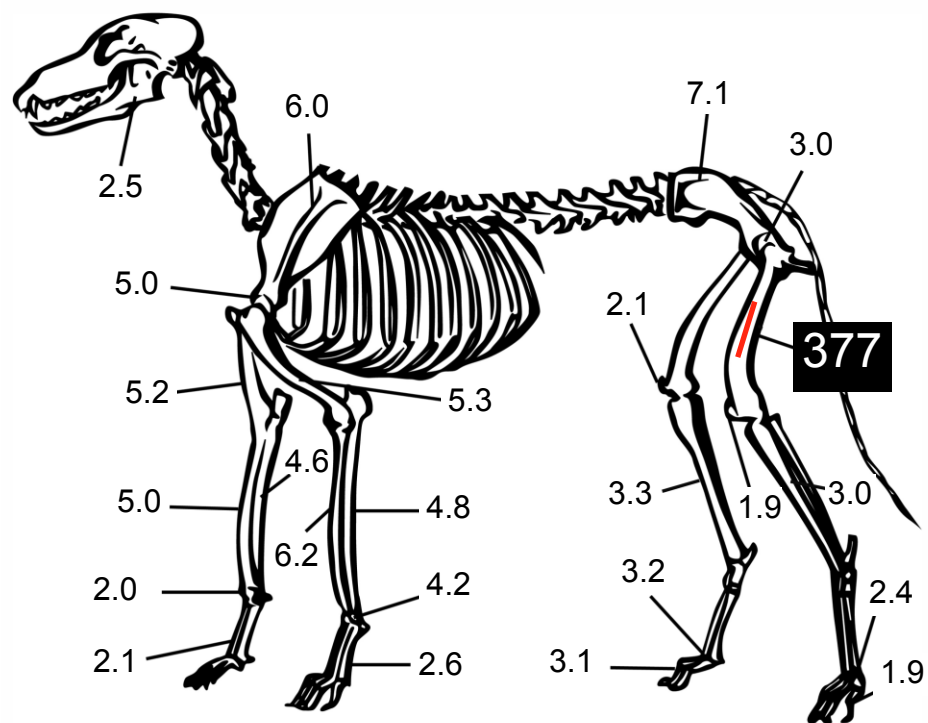


**Figure 14.** Skeletal distribution of zoledronic acid (ng/g dry bone). Average zoledronic acid concentration in peri-implant bone was 377 ng/g dry bone.

Tissue	Average mass zoledronic acid (ng/g tissue)
Heart	0.0
Kidney	0.0
Liver	0.0
Spleen	0.0
Lung	0.0
R. vastus lateralis	0.0
L. vastus lateralis	0.0
mandible	2.4
L. iliac crest	7.1
R. iliac crest	3.6
L. patella	1.9
R. patella	2.1
L. clavicle	6.0
R. clavicle	5.3
L. acetabulum	3.0
R. acetabulum	5.1
L. talus	2.4
R. talus	3.2
L. scaphoid	4.2
R. scaphoid	2.0
L. metatarsal	1.9
R. metatarsal	3.1
L. glenoid	5.0
R. glenoid	5.6
L. metacarpal	2.6
R. metacarpal	2.1
L. ulna	4.8
R. ulna	5.0
L. radius	6.2
R. radius	4.6
L. tibia	3.0
R. tibia	3.3
L. humerus	5.3
R. humerus	5.2
R. femur	5.2
L. femur (peri-implant bone)	377.2

**Table 1.** Average mass of zoledronic acid (in ng) per gram of tissue in all three dogs.

Mass zoledronic acid (ng/g tissue)			
Tissue	Dog 1	Dog 2	Dog 3
Heart	0.0	0.0	0.0
Kidney	0.0	0.0	0.0
Liver	0.0	0.0	0.0
Spleen	0.0	0.0	0.0
Lung	0.0	0.0	0.0
R. vastus lateralis	0.0	0.0	0.0
L. vastus lateralis	0.0	0.0	0.0
mandible	2.7	3.9	0.7
L. iliac crest	-	7.1	-
R. iliac crest	3.6	-	-
L. patella	1.5	0.6	3.5
R. patella	1.6	1.6	3.0
L. clavicle	5.2	6.8	0.0
R. clavicle	4.5	8.2	3.2
L. acetabulum	3.0	2.9	-
R. acetabulum	-	5.1	-
L. talus	2.3	2.5	-
R. talus	2.8	3.6	-
L. scaphoid	3.1	5.3	-
R. scaphoid	3.5	0.5	-
L. metatarsal	2.4	1.4	9.1
R. metatarsal	2.0	3.9	3.5
L. glenoid	4.8	5.3	-
R. glenoid	4.8	6.3	-
L. metacarpal	2.8	2.3	-
R. metacarpal	2.3	1.9	-
L. ulna	3.6	5.0	5.8
R. ulna	4.4	4.9	5.6
L. radius	4.1	5.6	8.8
R. radius	4.1	5.0	4.6
L. tibia	4.1	0.5	4.3
R. tibia	4.2	0.4	5.4
L. humerus	4.8	6.2	4.9
R. humerus	4.3	6.4	4.9
R. femur	4.2	6.2	5.1
L. femur (peri-implant bone)	349.3	329.5	452.7

**Table 2.** Mass of zoledronic acid (in ng) per gram of tissue in each of the three dogs. There are missing values because some tissues were not sampled. The concentration of zoledronic acid found in each bone varied between dogs but in all samples, the concentration of zoledronic acid was much less than in peri-implant bone.

The three right femora (i.e., the femora not containing an implant) were processed in their entirety, enabling a measurement of the total contained mass of zoledronic acid; these data are presented in Table 3. The amount of zoledronic acid detected in the three right femora ranged from 0.18  $\mu$ g to 0.28  $\mu$ g, with the mean of 0.21  $\mu$ g representing 0.21% of the starting dose. The mass of drug in each section of the right femora is shown in Figures 15-17. The indicated position of segments along the femora in Figures 15-17 is approximate.

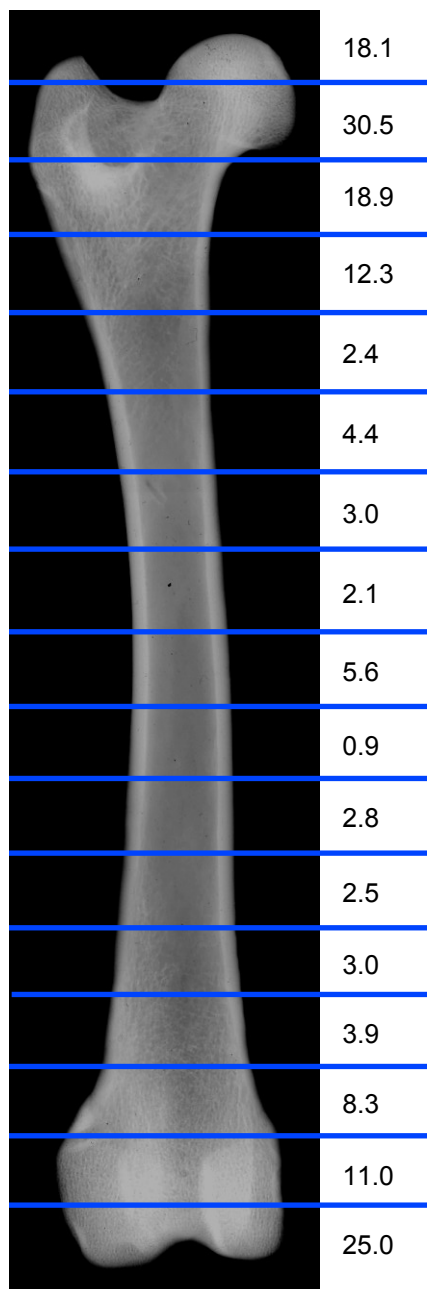
Dog 1	Dog 2	Dog 3	Average
0.18	0.28	0.18	0.21

**Table 3.** Total mass of zoledronic acid (in  $\mu$ g) in right femora.

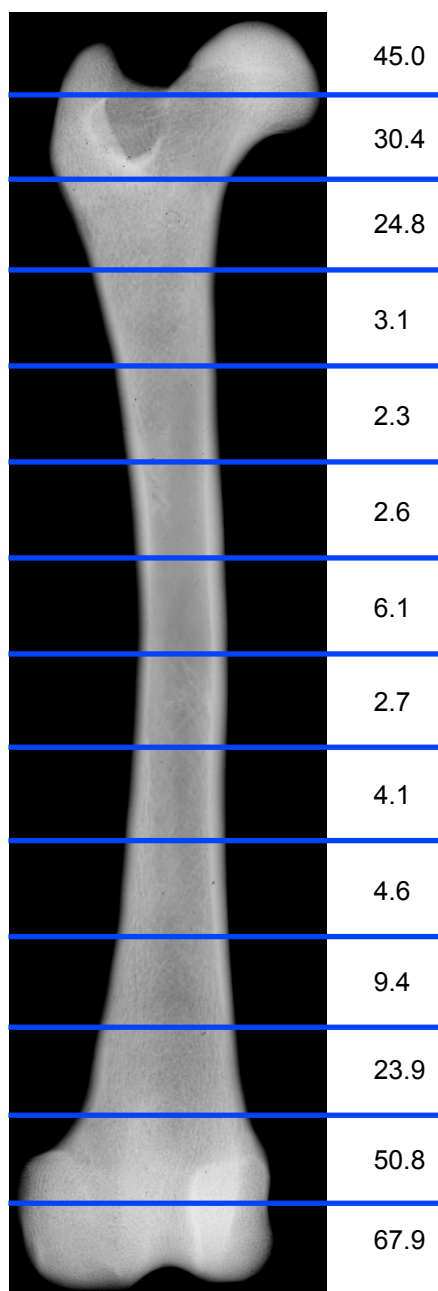
## 5.2 Implants and implant-containing femora

The only other bone processed in its entirety was one of the implant-containing femora (from Dog 3), which was sectioned and analyzed using liquid scintillation spectrophotometry. This allowed calculation of the total mass of zoledronic acid remaining in femoral bone, and also on and within the implant (Table 4). The total mass of zoledronic acid on and within the implant was 12.8  $\mu$ g, while the total mass in peri-implant bone was 4.4  $\mu$ g. The mass of zoledronic acid in the entire femur, including what was dissolved from the implant, was 19.2  $\mu$ g.

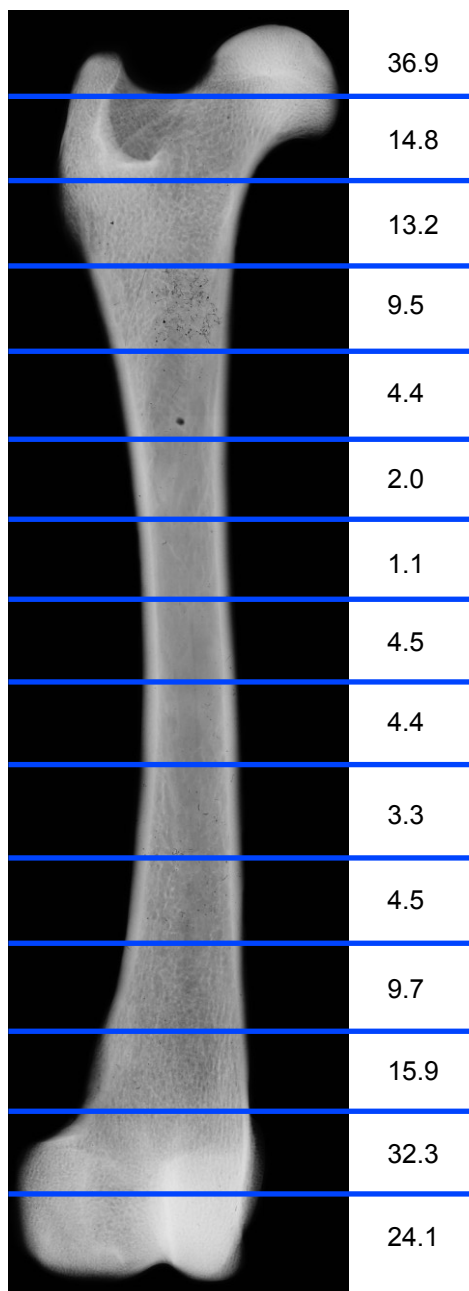




**Figure 15.** Zoledronic acid content (in ng) in each section of the right femur of Dog 1. Note the greater masses in the metaphyses compared to the diaphysis.



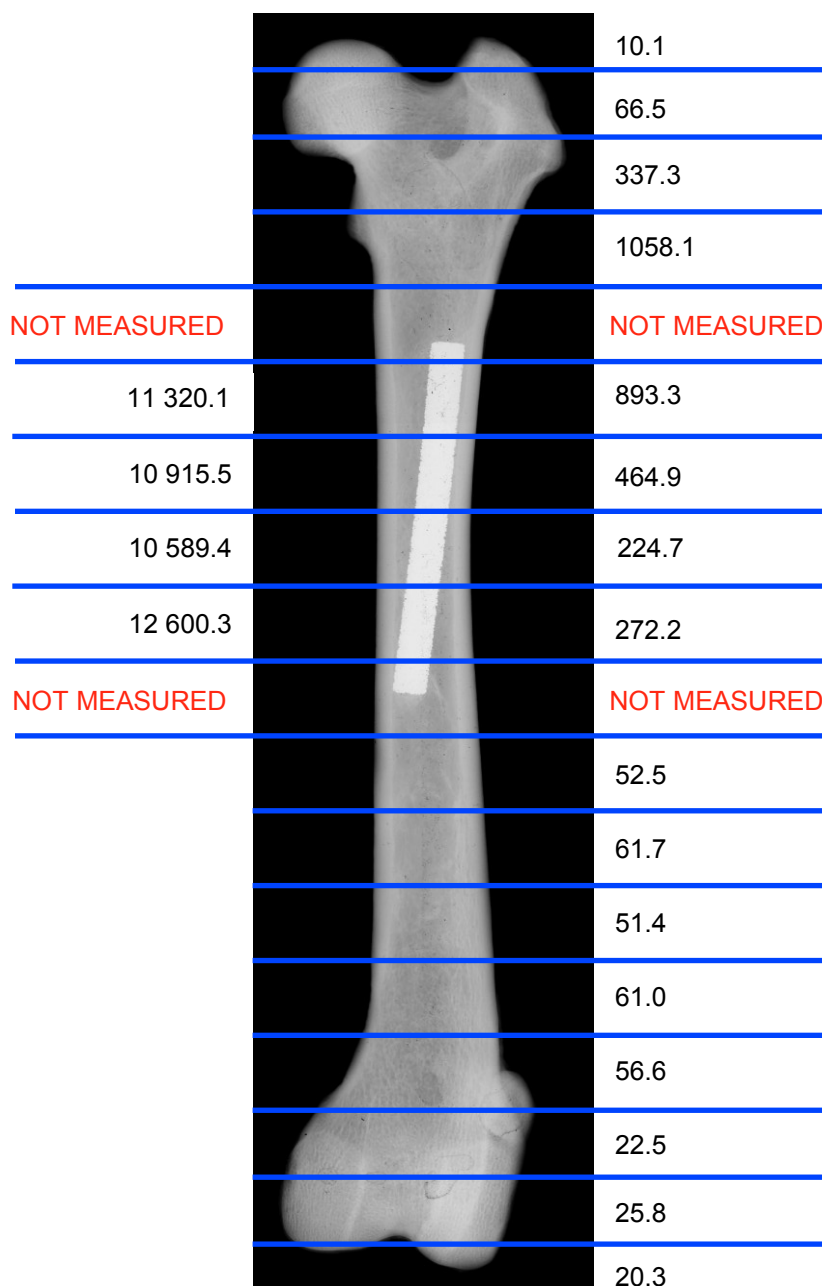
**Figure 16.** Zoledronic acid content (in ng) in each section of the right femur of Dog 2. Note the greater masses in the metaphyses compared to the diaphysis.



**Figure 17.** Zoledronic acid content (in ng) in each section of the right femur of Dog 3. Note the greater masses in the metaphyses compared to the diaphysis.

ng ZOLEDRONIC  
ACID ON AND  
WITHIN IMPLANT

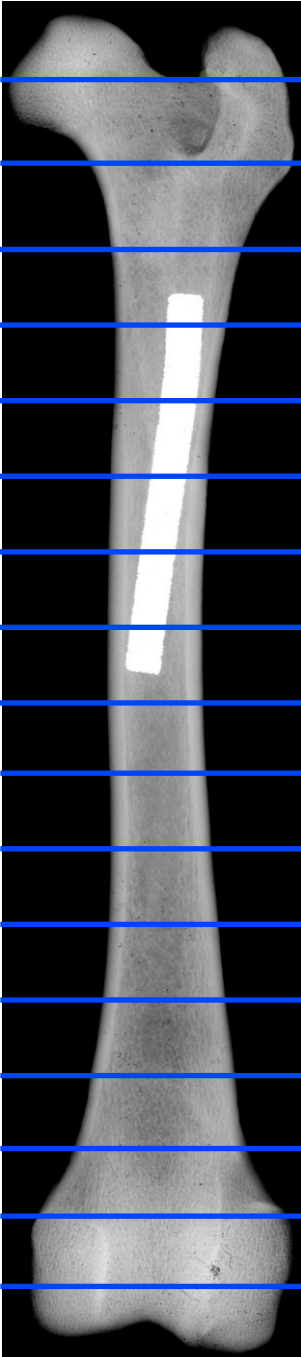
ng ZOLEDRONIC ACID  
IN PERI-IMPLANT  
BONE



**Figure 18.** Zoledronic acid content (in ng) in femoral bone and implant in Dog 1. The mass of zoledronic acid in proximal and distal sections of the implant and surrounding bone could not be quantified since these segments were embedded in acrylic and sectioned for analysis by autoradiography.

ng ZOLEDRONIC  
ACID ON AND  
WITHIN IMPLANT

ng ZOLEDRONIC ACID  
IN PERI-IMPLANT  
BONE

		48.1
		217.2
		459.2
NOT MEASURED		NOT MEASURED
9 024.8		757.1
7 582.2		553.1
6 409.4		437.0
7 251.7		208.5
NOT MEASURED		NOT MEASURED
		23.1
		19.4
		12.7
		8.75
		10.2
		25.5
		53.8
		59.8
		21.9

**Figure 19.** Zoledronic acid content (in ng) in femoral bone and implant in Dog 2. The mass of zoledronic acid in proximal and distal sections of the implant and surrounding bone could not be quantified since these segments were embedded in acrylic and sectioned for analysis by autoradiography. The implant appears to have deformed slightly upon insertion, but this would not have affected the results of this study.

ng ZOLEDRONIC  
ACID ON AND  
WITHIN IMPLANT

ng ZOLEDRONIC ACID  
IN PERI-IMPLANT  
BONE

		39.0
		75.0
		388.4
		1 272.6
2 492.5		1 733.0
2 004.9		807.0
2 005.1		551.8
2 279.7		543.5
2 803.4		508.0
1 209.1		253.1
		39.4
		25.8
		20.2
		19.7
		26.4
		84.4
		20.6

**Figure 20.** Zoledronic acid content (in ng) in femoral bone and implant in Dog 3. This was the only implant-containing femur for which the mass of zoledronic acid was quantified in all segments.

The proximal and distal implant-containing segments of the two remaining femora were analyzed using autoradiography. This meant that they could not be analyzed by liquid scintillation spectrophotometry and the mass of zoledronic acid in these segments could not be quantified. The mass of zoledronic acid in each femoral segment analyzed by liquid scintillation spectrophotometry is shown in Figures 18-20. The indicated position of segments along the femora in Figures 18-20 are approximate.

The average mass of zoledronic acid per centimeter of implant is shown for segments 2-5 in all dogs, and for segments 1-6 in Dog 3 (Table 5). The lengths of each implant segment are shown in Table 6. Segments were not cut to precise lengths. When all implant segments were measured (Dog 3), the lengths of the segments added to 4.6 cm whereas the length of the implant at the time of surgery was 5 cm. This material was lost during sectioning due to the thickness of the saw blade.

Dog	Mass ZA on/within implant (µg)	Mass ZA in left femoral bone (µg)	Mass in peri-implant bone (µg)	Total mass in femur including implant (µg)
Dog 3	12.8	6.4	4.4	19.2

**Table 4.** Mass of zoledronic acid on and within the implant, in peri-implant bone, and in the entire bone (excluding and including the implant). The mass of zoledronic acid in the left femurs of Dog 2 and Dog 1 could not be quantified since two segments from each femur were analyzed by autoradiography instead of liquid scintillation spectrophotometry.

	Average ug ZA/cm
Dog 1 (segments 2-5)	13.0
Dog 2 (segments 2-5)	8.3
Dog 3 (segments 2-5)	2.5
Dog 3 (segments 1-6)	2.9

**Table 5.** Average mass of zoledronic acid per centimeter of implant.

Dog	Implant segment	Segment length (cm)
1	2	0.82
	3	0.95
	4	0.89
	5	0.86
2	2	0.84
	3	0.86
	4	0.95
	5	1.05
3	1	0.65
	2	0.85
	3	0.90
	4	0.88
	5	0.95
	6	0.35

**Table 6.** Length of each implant segment analyzed using liquid scintillation spectrophotometry

The greatest concentrations of zoledronic acid were found in material dissolved off the implant. These materials included the hydroxyapatite coating and bone that had grown into the implant pores. Here the concentration of zoledronic acid was one to two orders of magnitude higher than at other skeletal sites. This is illustrated in Figure 21, where the distribution of zoledronic acid within femora containing an implant is shown graphically. Since two of the femora were each missing 2



segments, the amount of zoledronic acid in the missing sections was estimated to generate a continuous curve. The mass of drug in the missing segments was approximated by adding half of the amount of zoledronic acid found in one adjacent segment, to half the amount of zoledronic acid found in the other adjacent segment. The position of the implant in the radiographed femur in Figure 21 is meant to indicate the approximate position of the implant in each femur (based on measurements taken from each radiograph). In the proximal and distal ends of all femora containing an implant the concentration of zoledronic acid is comparable to that found at other skeletal sites (i.e., one to two orders of magnitude less than in peri-implant bone).

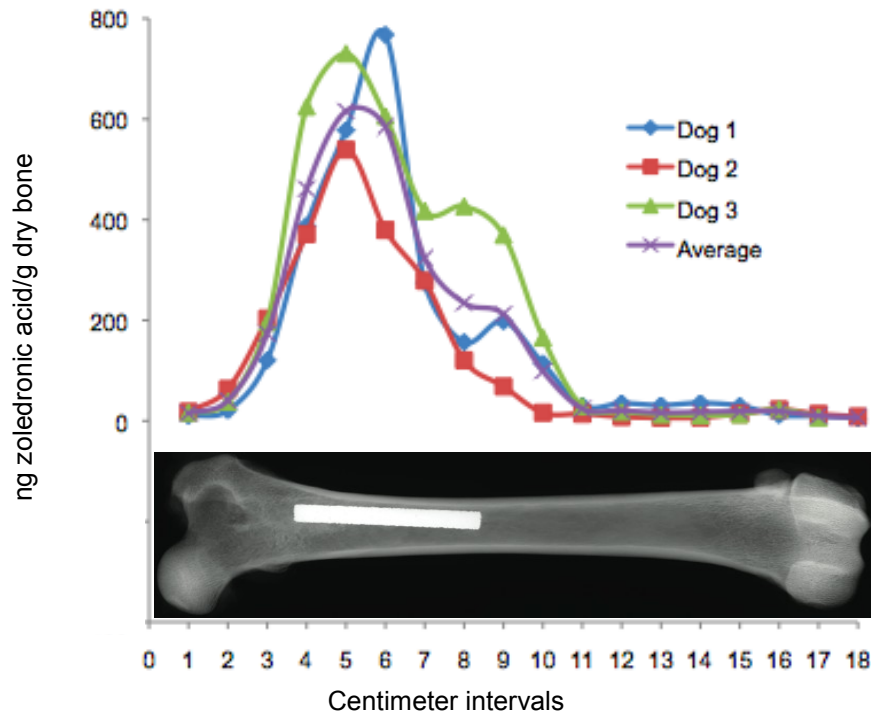


**Figure 21.** Graph illustrating zoledronic acid concentration as a function of centimeter intervals along the femur. Note the peak peri-implant zoledronic acid concentration around the proximal half of the implant. Peri-implant bone possessed one to two orders of magnitude more zoledronic acid than bone slightly proximal or distal to the implant.

### 5.3 Analysis of defatting and dehydrating solutions

No radiation was detected in either the alcohol or ether-acetone solutions used to defat and dehydrate the samples.

### 5.4 Autoradiography

The results of the autoradiography portion of the study are illustrated in Figures 22-25. In the series of proximal and distal bone-implant sections little to no zoledronic acid was apparent within the cortical bone surrounding the implant. A faint rim can be seen partially lining the endosteal side of the cortex in most sections. In some sections from distal

ends of both implants, and the proximal end of the implant of Dog 2 there appears to be a very small amount of zoledronic acid on the outer edge of the cortical bone (indicated by arrows). In all cases, the greatest concentration of zoledronic acid was on or within the implant. In one proximal section from Dog 2 and two distal sections from Dog 1 implants appeared blurred and the pores of the implant were not visible. In autoradiographs of sections from both dogs, the concentration of zoledronic acid visibly declined with increasing distance from either end of the implant (the physical distance between sections is about 1 mm). Even when the implant was no longer present in contact radiographs, the corresponding autoradiographs showed some zoledronic acid remaining in trabecular bone in the femoral canal, around the endosteal side of the cortex, and, in all but the proximal sections from Dog 1, around the periosteal side of the cortex.

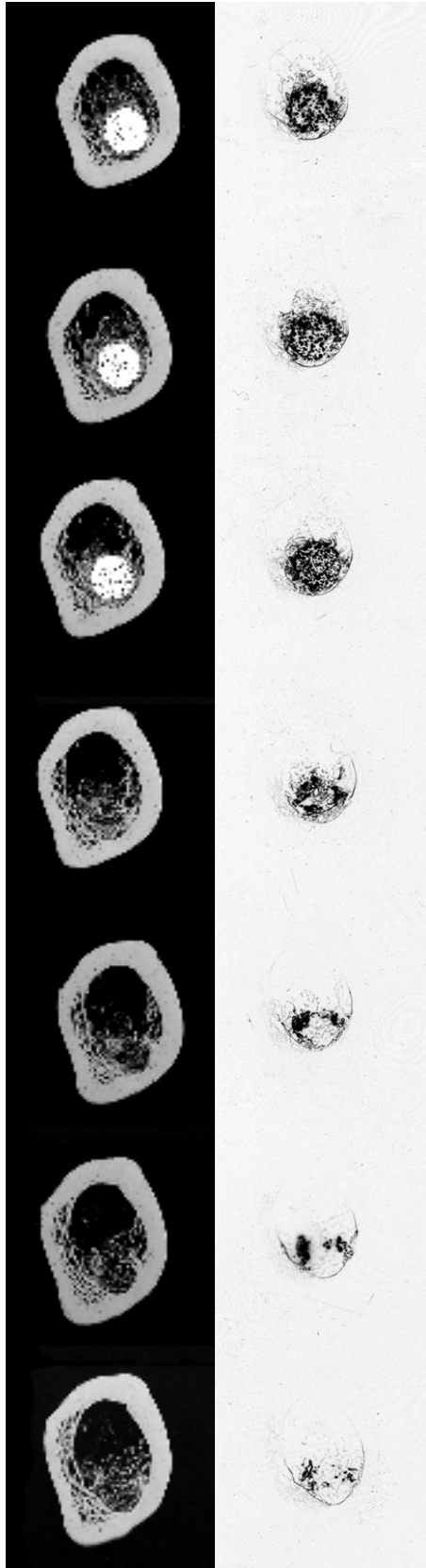


**Figure 22.** Proximal serial sections of implant and surrounding bone from Dog 1 imaged in a contact radiograph (left) and a corresponding autoradiograph (right). The implant is present in the top three sections. The autoradiography reveals that zoledronic acid is strongly concentrated in and around the implant with diminished content distal to the implant and in surrounding bone.

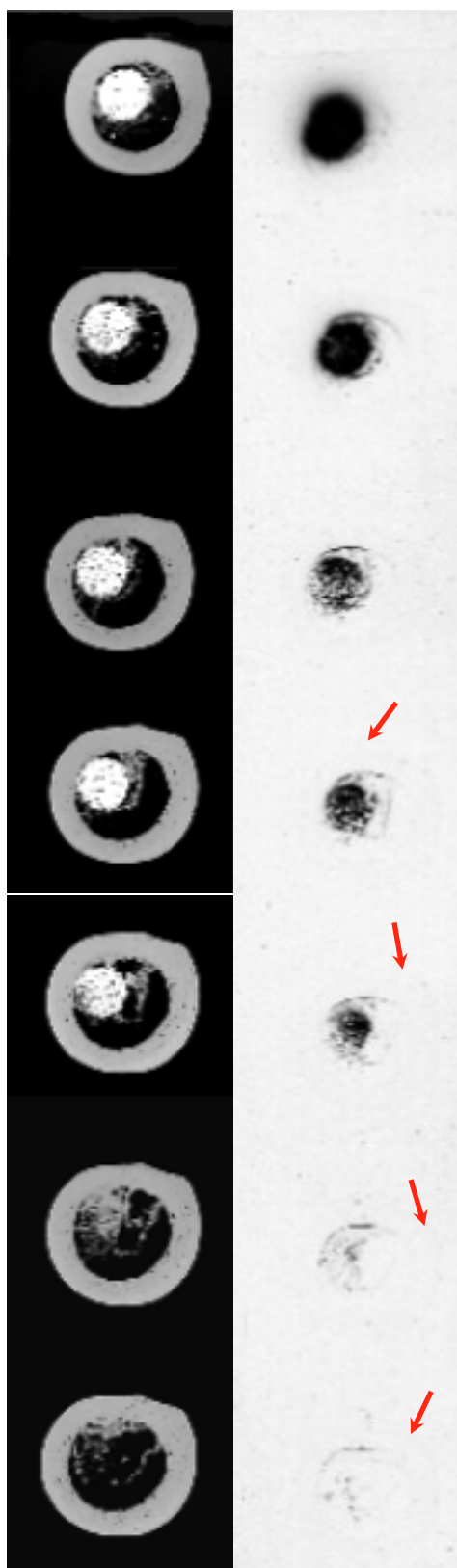


**Figure 23.** Distal serial sections of implant and surrounding bone from Dog 1 imaged in a contact radiograph (left) and a corresponding autoradiograph (right). The implant is present in the top five sections. The autoradiography revealed that zoledronic acid was strongly concentrated in and around the implant with diminished content distal to the implant and in surrounding bone. Zoledronic acid around the outer edge of the cortex is indicated by arrows.

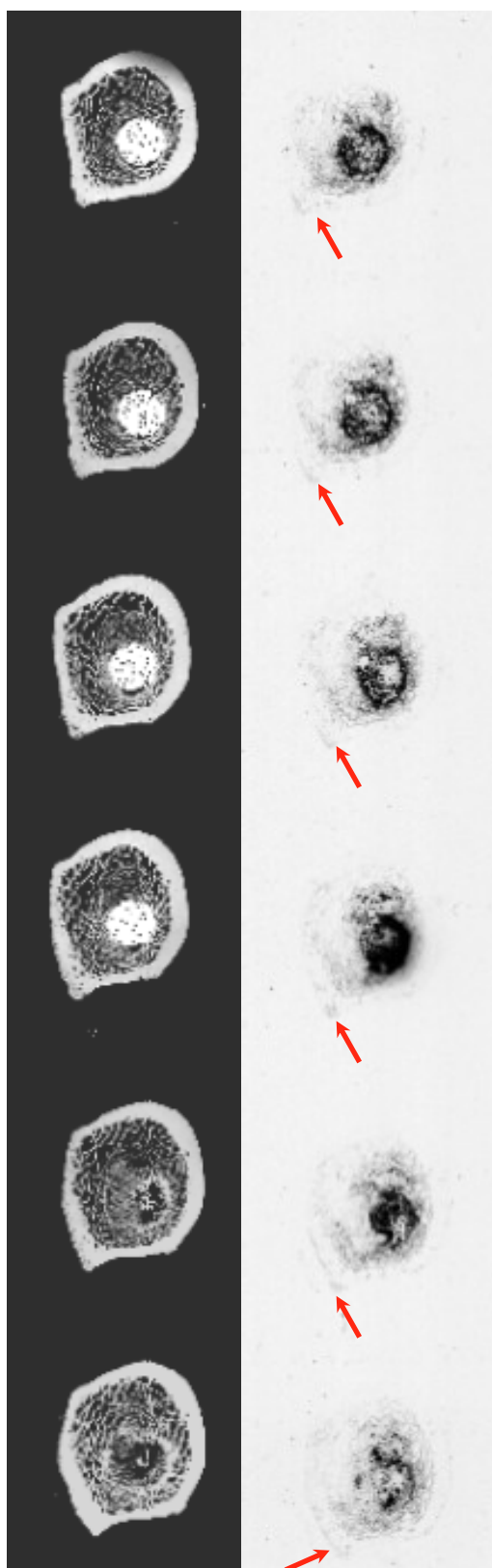


**Figure 24.** Proximal serial sections of implant and surrounding bone from Dog 2 imaged in a contact radiograph (left) and a corresponding autoradiograph (right). The implant is present in the top four sections. The autoradiography revealed that zoledronic acid was strongly concentrated in and around the implant with diminished content distal to the implant and in surrounding bone. Zoledronic acid around the outer edge of the cortex is indicated by arrows.

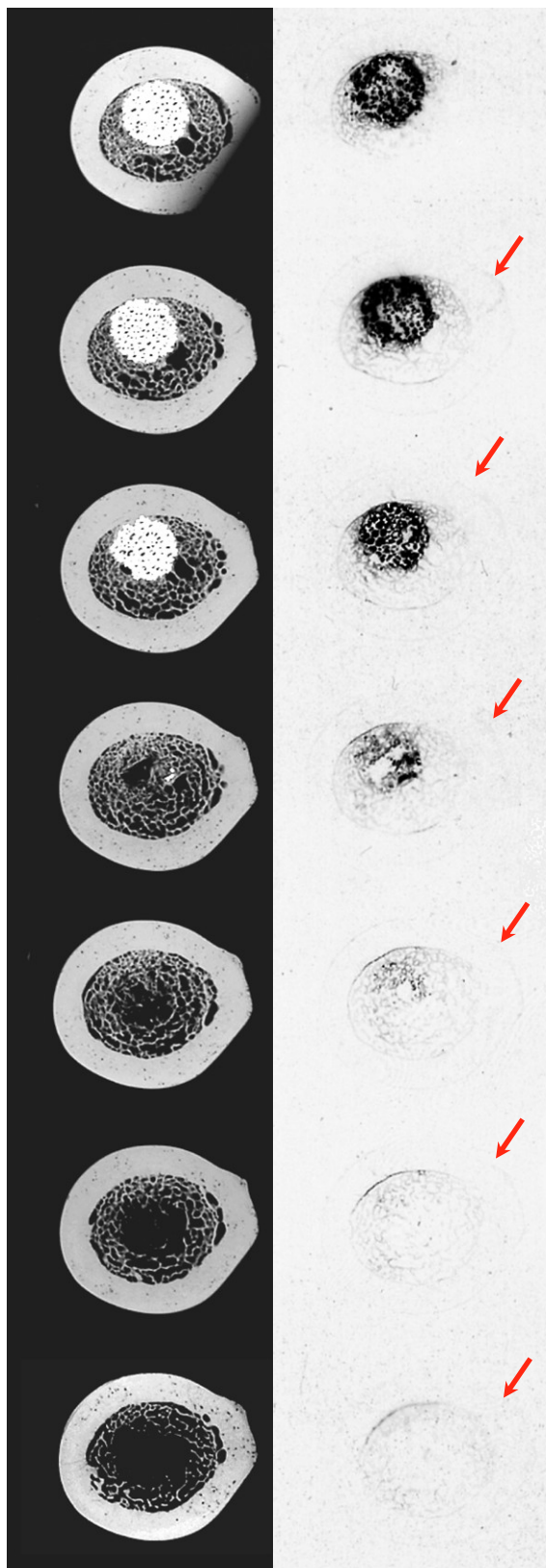


**Figure 25.** Distal serial sections of implant and surrounding bone from Dog 2 imaged in a contact radiograph (left) and a corresponding autoradiograph (right). The implant is present in the top three sections. The autoradiography revealed that zoledronic acid was strongly concentrated in and around the implant with diminished content distal to the implant and in surrounding bone. Zoledronic acid around the outer edge of the cortex is indicated by arrows. The top section on the left appears incomplete because it was obliquely oriented within the embedding medium and was thus sectioned at an angle.

## **6.0 DISCUSSION**

---

The results of the experiments presented herein indicate that  $^{14}\text{C}$ -labeled zoledronic acid eluted from the surface of an implant remains mainly local to the implant. This localization has been shown in two ways. First, liquid scintillation counting of bone samples immediately next to the implant revealed drug concentrations two to three times higher than what was found in bone samples slightly distant from the implant. Second, qualitative autoradiography showed substantial drug on and within the implant, but less in peri-implant bone and very little or none was seen in cortical bone beyond the endosteum. Using radiolabeled bisphosphonate to detect drug distribution to bone and soft tissue samples using liquid scintillation proved to be relatively simple and effective. Using thin bone-implant sections to image the location of  $^{14}\text{C}$ -labeled zoledronic acid using autoradiography techniques was similarly simple and effective.

### **6.1 Distribution of zoledronic acid**

The finding of zoledronic acid in the skeleton was evidence that zoledronic acid does indeed become distributed systemically when delivered from an implant. Presumably the drug was distributed by diffusing into the circulation, although exactly what transport mechanism was involved or at what rate this occurred is unknown at this point. Closer to the implant, zoledronic acid may have also been transported via local osteoclast activity (66). The absence of the drug in soft tissues was



expected since it is known to accumulate in osseous tissues due to its high affinity for calcium. Zoledronic acid that was distributed to other parts of the skeleton was detected at very low levels - an unsurprising finding given that the drug is rapidly excreted once it reaches the circulatory system (up to 90% is excreted in the urine 48 hours after administration). These levels were slightly lower in the diaphysis of long bones as compared to metaphyses where there is more cancellous bone and hence greater bone surface area.

The images obtained by autoradiography provided further qualitative evidence that zoledronic acid remained local. In Figures 22-25 there was clearly more drug on and within the implant than there was in peri-implant bone where it appeared absent or nearly absent. The majority of zoledronic acid remaining at the implant site was likely to be either bound to the hydroxyapatite coating, or incorporated into bone that had grown into the implant pores. It is unclear from this study how accessible this remaining drug would be to peri-implant bone.

Based on visual examination, there did not appear to be a large difference between proximal and distal sections imaged using autoradiography. Two of the distal sections from Dog 1 (top two in Figure 23) appear blurred and the implant struts were obscured by intense black staining. This would seem to indicate that there was more drug present on and within this section of implant. Closer inspection of the embedded section revealed that it was roughly twice the thickness of the other sections. This added thickness may have led to greater exposure of the

film and hence the darker staining. However, one of the proximal sections from Dog 2 (fourth from the top in Figure 24) also exhibited blurring and strut-obscuring blackness, yet the thickness of this section was not different from other sections. An alternative explanation for the intense staining in these sections could simply be that the concentration of zoledronic acid was higher due to differences in local bone metabolism, uneven doping of the implant prior to insertion, or displacement of the drug upon insertion of the implant (see below).

Qualitative examination of sections revealed that the radial distribution of zoledronic acid differed between Dog 1 and Dog 2. Slightly more zoledronic acid was noted around the outer surface of the cortex in sections from Dog 2 as compared to Dog 1. To determine if these differences are significant, more dogs would need to be studied, and the concentration of drug as a function of distance radially from the implant would need to be quantified. It seems reasonable to attribute the different distributions to differences in bone metabolism between the two dogs.

The distribution of zoledronic acid within the implant-containing femurs was quantified and depicted in Figure 21. These graphs indicated that there was a sharp rise and fall in zoledronic acid content immediately around the implant compared to the proximal and distal ends of the femur. The values of the data points used to construct the graphs are shown in Figures 18-20. It is interesting to note that the graphs in Figure 21 are slightly skewed such that the concentration of zoledronic acid peaked near the proximal end of the implants compared to the distal end. Although care

was taken to ensure the implant was evenly coated with zoledronic acid, this distribution may have changed somewhat when the implant was inserted into the femoral canal. As the implant was tapped into position, the surface of the implant would have scraped the surface of the reamed bone channel. This may have caused some of the zoledronic acid at the distal end to be mechanically dislodged and displaced proximally.

There is a second possible explanation for the skewed zoledronic acid distribution. The implant was seated in the canal to the distal extent of the reaming. This left a void above the implant from the initial reaming bounded by the implant on the distal side and by bone wax used to fill the initial hole on the proximal side. Canal bleeding due to the surgery caused this void to fill with blood. Any radioactive material in the blood would then have been trapped between the implant and the bone wax at the entry hole. Thus the slightly skewed distribution of zoledronic acid along the implant may just have represented an artifact of implantation rather than actual elution and distribution. Regardless, there was a sharp attenuation in zoledronic acid concentration within one or two centimeters remote from the implant.

In addition to the qualitative and quantitative evidence described herein, an elution study by Peter et al (66) supports our observations that zoledronic acid that elutes from an implant remains local. In rats that received hydroxyapatite- and zoledronic acid-coated implants, changes in bone density were observed that varied with distance from the implant and dose. The highest dose resulted in a low bone density within a radius 20

μm from the implant due to impaired mineralization, but resulted in increased bone density 200 μm from the implant due to what they described as a dilution of the drug with increasing distance. Lower doses resulted in higher bone density near the implant and decreasing bone density with increasing distance from the implant.

## **6.2 Distribution at sub-therapeutic levels**

Although skeletal distribution of zoledronic acid was found to be small, it is important to consider whether the amount of drug distributed is below the threshold required to elicit clinically significant effects. In this study, the concentration of zoledronic acid in peri-implant bone was 53-fold to almost 200-fold greater than the concentration found elsewhere in the skeleton. It would be impossible to know for certain, given the sum of all available information, if these levels were sub-therapeutic, but given that zoledronic acid concentration in bone other than peri-implant bone was so much lower it seems unlikely that drug distributed at such low levels would have a clinically relevant effect. If some effect were to occur in parts of the body distant to the implant, these effects could reasonably be expected to be mild if not negligible. This is important because of both the adverse effects that some patients experience with systemic exposure to zoledronic acid and because of the unknown long-term effect of bisphosphonates on the mechanical properties of bone, issues that were discussed in Chapter 2 (Literature Review). Future studies should examine implants dosed with varying amounts of zoledronic acid to

determine the minimum dose needed to obtain clinically desirable results. Given the high degree of zoledronic acid localization demonstrated in this study, such studies may employ bilateral models with suitable controls for comparison. It would also be informative to determine the correlation between concentrations of zoledronic acid in the skeleton and the side effects sometimes associated with the use of this drug.

### **6.3 Elution of zoledronic acid from coated implants**

While the systemic distribution of zoledronic acid may be low enough to avoid adverse effects, the manner in which the drug is released may help determine how effective this form of treatment is. Although it remains unclear what elution characteristics are best for this type of application, an elution profile for the type of implants used in this study has been described by Roberts (68). Roberts coated  $^{14}\text{C}$ -labelled zoledronic acid onto porous tantalum implants with and without a plasma sprayed hydroxyapatite coating. These implants were identical to the ones used in this thesis. Roberts placed the implants into vials of water and sampled the water at 5, 15, and 30 minutes, 1, 3, 12, and 24 hours, 1 week, and then weekly until 12 weeks. Within 5 minutes, 34% of the drug was released from hydroxyapatite coated implants (Figure 26). That amount rose to 50% after 12 hours with a much slower release rate thereafter. After 12 weeks, 55% of the original amount of drug placed on implants was released. In contrast, when implants were not coated with

hydroxyapatite, roughly 97% of zoledronic acid was released within 5 minutes and all was released after 15 minutes.

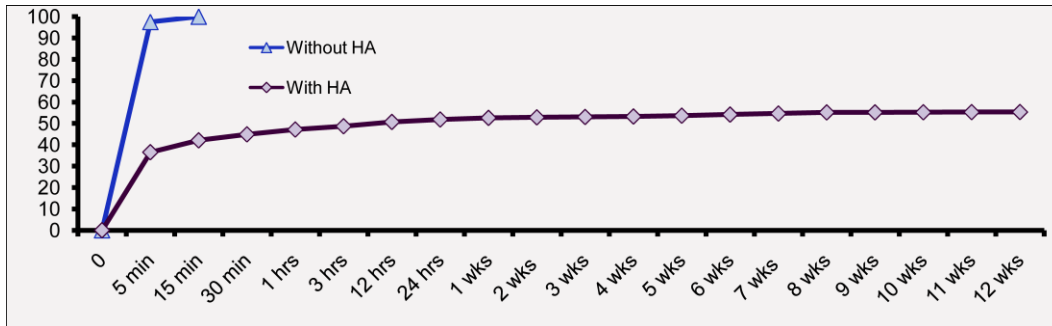


**Figure 26.** Release rate of zoledronic acid from implants with or lacking a hydroxyapatite coating. Elution was done in water. All zoledronic acid was released from implants without a hydroxyapatite coating within 15 minutes. Note the initial burst release of zoledronic acid from hydroxyapatite-coated implants followed by a plateau out to 12 weeks. Image taken from Roberts, 2008.

In Roberts' study, the rapid release of zoledronic acid from implants not coated with hydroxyapatite was predictable; without a calcium-based coating to chemically bind zoledronic acid to the implant surface, the drug was quickly hydrated and released into solution. There was also an early burst release of zoledronic acid from hydroxyapatite-coated implants, despite the known chemical affinity of bisphosphonate for hydroxyapatite. There are two possible explanations for the biphasic release profile from porous implants reported by Roberts. When hydroxyapatite is plasma sprayed onto a porous implant, only the outer surface of the outer struts are coated; the inner strut surfaces remain uncoated (Figure 27). When zoledronic acid was applied to the implants used in both this study and

Roberts' study, it was applied by hand onto the implant surface (Figure 6). Some of the drug became bound to the hydroxyapatite surface coating while the remainder wicked through surface tension throughout the pores and onto the bare surface of the inner struts where the zoledronic acid was bound only weakly by ionic interactions with tantalum. The drug that was released within the first 12 hours from hydroxyapatite-coated implants is reasonably presumed to be drug that was weakly bound on the inner tantalum struts. The plateau region of the curve likely represents zoledronic acid that remained more tightly bound by the hydroxyapatite coating.

The second possible explanation is that the hydroxyapatite coating may have become saturated with zoledronic acid at some point. Any additional zoledronic acid present once the saturation point was reached may have been weakly bound on the surface of the hydroxyapatite and easily hydrated once the implant was placed in water. The lack of a chemical bond holding the extra zoledronic acid in place would likely make the drug more accessible to osteoclasts. Although there are no published data reporting the saturation point of hydroxyapatite with zoledronic acid, there is some evidence to support this explanation. Roberts performed the same elution study described above using solid, grit-blasted implants without any three-dimensional struts or pores. In the absence of a hydroxyapatite coating all of the zoledronic acid was released within 24 hours. However, with a hydroxyapatite coating deposited on the grit-blasted surface Roberts reported a biphasic release profile similar to that

seen with porous implants. In this case, 50% was eluted after 15 minutes and 80% was eluted after 3 weeks. The early burst release of zoledronic acid observed with these implants could not have come from metallic surfaces that were uncoated with hydroxyapatite. This suggests that the early burst release was due to rapid hydration of unbound surplus zoledronic acid on the hydroxyapatite surface.

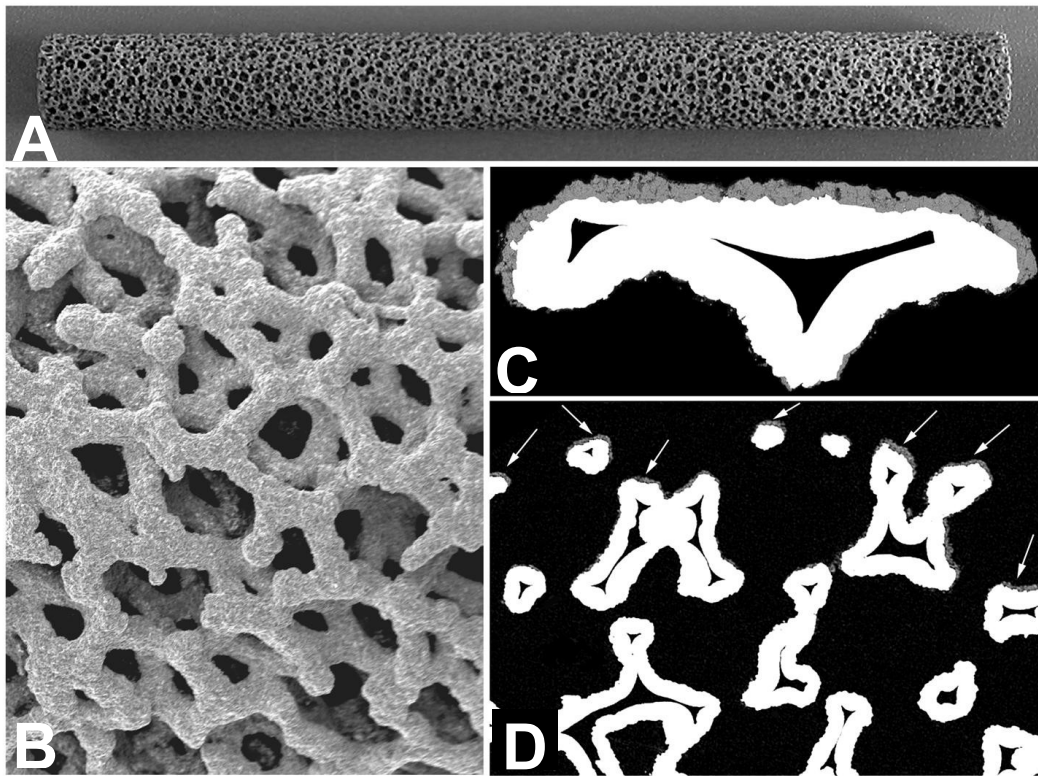


**Figure 27.** A porous tantalum implant plasma spray coated with hydroxyapatite is shown in A while a scanning electron micrograph of the surface is shown in B. Back-scattered scanning electron micrographs of cross-sections of the implant (C and D) show the distribution of plasma-sprayed hydroxyapatite on the implant surface. In C and D, tantalum struts appear white while hydroxyapatite appears grey. It is evident that plasma sprayed hydroxyapatite reaches only the outer surface of the implant's outer struts (indicated by white arrows).



Without further investigation, it is difficult to say with certainty which explanation applied to elution from implants used in this thesis or whether a combination of the explanations was responsible. Assuming the elution curves generated by Roberts (68) accurately reflected in vivo conditions, the implants studied for this thesis should have retained approximately 45  $\mu\text{g}$  of zoledronic acid (45% of the original dose, based on the 12 week elution curve in Figure 26). In Dog 3, the only dog in whom the total mass of femoral zoledronic acid was quantified, only 12.8  $\mu\text{g}$  remained. Although definitive conclusions cannot be drawn based on data for a single dog, it is possible that more of the drug was released from hydroxyapatite after one year compared to the 12 week interval investigated by Roberts. It is also quite likely that the elution rate is different in the physiological environment than in water. Even though the mass of zoledronic acid remaining on the implants from Dog 1 and Dog 2 could not be fully quantified (due to retention of proximal and distal segments for the autoradiography studies), it is interesting to compare the mass remaining on segments 2-5 of these implants. The total mass of zoledronic acid in implant segments 2-5 for Dog 1 was 45.0  $\mu\text{g}$  and for Dog 2 was 30.3  $\mu\text{g}$  - values much closer to what would be predicted from the elution curve in Figure 26. Variability in retained zoledronic acid between implants has also been described by Roberts (68), who performed the same distribution experiment described here but with tissue harvest after six weeks rather than one year. Roberts did not image femurs using autoradiography and was thus able to

calculate a total mass of zoledronic acid remaining in the three implants that were examined (19.4 µg, 19.6 µg, and 44.6 µg).

Although Roberts was unable to identify the cause of the variation in her experiments, there could be several reasons for the variability seen between implants both in her study and in the present thesis. With such a small sample size it is possible that normal variation between animals is responsible. Differences in bone metabolism between dogs is a potential source of variability since sites of active bone resorption will incorporate more bisphosphonate than less active sites (34). Also, the assumption in this study was that zoledronic acid was evenly distributed onto the implant surface. Care was taken to achieve this but it is possible that the drug was not evenly distributed between the hydroxyapatite and exposed tantalum struts. Alternatively, the large amounts of drug remaining on the implant could be due to extra zoledronic acid-containing bone remaining on these implants; either more bone grew into the implant pores, or more bone was removed from some implants than others during the processing stages. Since bone was manually scraped off the surface of the implant, this could be a source of the large variability. However, if this were the case there should have been a correspondingly larger mass of zoledronic acid in the peri-implant bone (all bone that was manually scraped off the periphery of the implant segments was included with the rest of peri-implant bone in the measurements of mass of contained zoledronic acid). This was not the case (Figures 18-20).

Increasing the sample size might have provided a stronger indication of the source of inter-animal variability. However, the purpose of this study was not to determine statistical differences between the different measured parameters. Rather it was simply designed to provide a general indication of whether or not or to what extent there was systemic distribution of locally delivered bisphosphonate. As shown in Table 2 there is variability in the amount of zoledronic acid found in various bone. What is important to note is that all of these levels were very low.

In the present study, analysis of defatting and dehydrating solutions indicated that no zoledronic acid was lost to these processing steps. Roberts (68), however, reported the presence of small quantities of zoledronic acid in the ether-acetone solutions used to defat her samples. She recovered an average of 0.37 µg of zoledronic acid from defatting solutions for each animal, indicating that some zoledronic acid had been present in the fatty substance of the bone marrow. The only difference in protocol between these two studies was the time between implantation and tissue harvest. Since Roberts tested samples after six weeks and samples for the present study were tested after one year, it would appear that any zoledronic acid delivered to the fatty substance of the bone marrow is in some manner eliminated or redistributed with increased time.

The data collected for the present study, together with Roberts' (68) six week data, represent the first reported measurements of local and skeletal distribution from a bisphosphonate-eluting orthopaedic implant. To date, no one has established a standard way of measuring how much drug

remains in the body and on the implant. Quantifying the mass of zoledronic acid remaining on implants and in skeletal tissues, as was done in this study, is one way to measure distribution and elution. However, since hydroxyapatite as well as bone was dissolved off the implant and analysed in the same solution there was no way to determine how much zoledronic acid remained in hydroxyapatite and how much had been incorporated into bone attached to the implant. Since a standard way of measuring how much drug remains has not yet been established, the mass of zoledronic acid per centimeter of implant is presented in Table 5. This may also be a relevant form of analysis since it takes into consideration the length of bone exposed to the bisphosphonate.

#### **6.4 Optimizing drug elution**

If we can optimize how a drug elutes from an implant, we should be able to maximize the effectiveness of this form of implant design. But many questions remain about the best elution profile a drug-eluting implant should have. Is an initial burst release followed by a plateau best? Or would an immediate and complete release be better? Perhaps a more gradual release would be ideal, but over what period of time should it occur? Roberts examined elution in water, but elution in saline or serum may more accurately represent the local environment around an implant. Different elution profiles could be achieved using different formulations of calcium phosphate that have different dissolution rates. Tricalcium phosphate, for example, degrades more rapidly than hydroxyapatite (69)

which may result in a faster or more complete release of zoledronic acid. Since early fixation is necessary to maintain long-term fixation, it may be beneficial to release zoledronic acid immediately and completely soon after implantation. Conversely, if zoledronic acid is still present and available to bone one year or more after implantation, it may be useful in preventing late loosening or fracture. Late peri-prosthetic fractures have been reportedly increasing according to the Swedish National Hip Arthroplasty Register (70). Not only is this complication costly, it is associated with a high morbidity. A different elution profile may also be obtained by using solid implants, or a technique other than plasma spraying to ensure all surfaces of a porous implant are coated with hydroxyapatite. The variability observed in this study highlights the need for more elution studies in the future, using implants with different calcium phosphate formulations and surface characteristics. Regardless of these characteristics, the results of this thesis indicate that the eluted bisphosphonate will largely remain localized to the implant site, with minimal systemic distribution.

## **7.0 CONCLUSION**

---

This study provided valuable insight into how zoledronic acid that is locally eluted from an implant binds to adjacent bone and becomes distributed systemically. The data clearly demonstrated that zoledronic acid remained very local when eluted from a hydroxyapatite-coated porous implant. Minute amounts escaped into the circulation and were systemically distributed but at levels that were likely to be sub-therapeutic. This is supported by the observation in ancillary studies that increases in net bone formation around zoledronic acid-dosed porous tantalum implants are very much confined to the immediate peri-implant space, where the zoledronic acid concentration was measured in this study to be two orders of magnitude greater than in remote sites of the skeleton. The fact that there is very little escape of zoledronic acid from the implant also justifies the use of bilateral implant models that compare control with zoledronic acid-eluting implants. In conclusion, these data support the concept of local bisphosphonate delivery and show that the risk of systemic side effects and unnecessary skeletal remodelling is minimal.

## 8.0 REFERENCES

---

1. Patient Demographics. American Academy of Orthopaedic Surgeons website. <http://www.aaos.org/research/stats/patientstats.asp>. Accessed April 28, 2009.
2. United States Bone and Joint Decade: *The Burden of Musculoskeletal Diseases in the United States*. Rosemont, IL; American Academy of Orthopaedic Surgeons; 2008.
3. Berry DJ, Harmsen WS, Cabanela ME, Morrey BF. Twenty-five-Year Survivorship of Two Thousand Consecutive Primary Charnley Total Hip Replacements. *J Bone Joint Surg*. 2002; 84-A(2): 171-177.
4. Callaghan JJ, Albright JC, Goetz DD, Olejniczak JP, Johnston RC. Charnley Total Hip Arthroplasty with Cement: Minimum Twenty-five-Year Follow-up. *J Bone Joint Surg Am*. 2000; 82: 487-497.
5. Morshed S, Bozic KJ, Ries MD, Malchau H, Colford JM Jr. Comparison of cemented and uncemented fixation in total hip replacement: A meta-analysis. *Acta Orthopaedica*. 2007; 315-326.
6. Engh CA, Bobyn JD, Glassman AH. Porous-coated hip replacement: The factors governing bone ingrowth, stress shielding, and clinical results. *J Bone Joint Surg*. 1987; 69B: 45-55.
7. Park SH, Llinás A, Goel VK. Bone Repair and Joint Implants. In: Bronzino JD, ed. *The Biomedical Engineering HandBook*. 2nd ed. Boca Raton: CRC Press LLC; 2000.
8. Bobyn JD, Pilliar RM, Cameron HU, Weatherly GC. The optimum pore size for the fixation of porous-surfaced metal implants by the ingrowth of bone. *Clin Orthop Relat Res*. 1980; 150: 263-270.
9. Kienapfel H, Sprey C, Wilke A, Griss P. Implant Fixation by Bone Ingrowth. *J Arthrop*. 1999; 14(3): 355-368.
10. Feighan JE, Goldberg VM, Davy D, Parr JA, Stevenson S. The influence of surface-blasting on the incorporation of titanium-alloy implants in a rabbit intramedullary model. *J Bone Joint Surg Am*. 1995; 77: 1380-1395.
11. Shalabi MM, Gortemaker A, Van't Hof MA, Jansen JA, Creugers NHJ. Implant Surface Roughness and Bone Healing: a Systematic Review. *J Dent Res*. 2006; 85(6): 496-500.

12. Sullivan DY, Sherwood RL, Mai TN. Preliminary results of a multicenter study evaluating a chemically enhanced surface for machined commercially pure titanium implants. *J Prosthet Dent*. 1997; 78: 379-386.
13. Wong M, Eulenberger J, Schenk R, Hunziker E. Effect of surface topology on the osseointegration of implant materials in trabecular bone. *J Biomed Mater Res*. 1995; 29: 1567-1575.
14. Black J. Biological Performance of Tantalum. *Clin Mater*. 1994; 16: 167-173.
15. Bobyn JD, Stackpool GJ, Hacking SA, Tanzer M, Krygier JJ. Characteristics of bone ingrowth and interface mechanics of a new porous tantalum biomaterial. *J Bone Joint Surg [Br]*. 1999; 81-B: 907-914.
16. Bobyn JD, Poggie RA, Krygier JJ, et al. Clinical Validation of a Structural Porous Tantalum Biomaterial for Adult Reconstruction. *J Bone Joint Surg Am*. 2004; 86: 123-129.
17. de Groot K, Wolke JG, Jansen JA. Calcium phosphate coatings for medical implants. *Proc Inst Mech Eng H*. 1998; 212(2): 137-147.
18. Puleo DA, Nanci A. Understanding and controlling the bone-implant interface. *Biomaterials*. 1999; 20: 2311-2321.
19. Hacking SA, Tanzer M, Harvey EJ, Krygier JJ, Bobyn JD. Relative Contributions of Chemistry and Topography to the Osseointegration of Hydroxyapatite Coatings. *Clin Orthop Rel Res*. 2002; 405: 24-38.
20. Elmengaard B, Bechtold JE, Søballe K. *In vivo* effects of RGD-coated titanium implants inserted in two bone-gap models. *J Biomed Mater Res*. 2005; 75A: 249-255.
21. Pilliar RM, Lee JM, Maniopoulos C. Observations on the Effect of Movement on Bone Ingrowth into Porous-Surfaced Implants. *Clin Orthop Rel Res*. 1986; 208: 108-113.
22. Morra M. Biochemical modification of titanium surfaces: Peptides and ECM proteins. *Eur Cell Mater*. 2006; 12: 1-15.
23. Leknes KN, Yang J, Qahash M, Polimeni G, Susin C, Wikesjo UME. Alveolar ridge augmentation using implants coated with recombinant human bone morphogenetic protein-7 (rhBMP-7/rhOP-1): radiographic observations. *J Clin Periodontol*. 2008; 35: 914-919.



24. Burke DW, Bragdon CR, O'Connor DO, et al. Dynamic measurement of interface mechanics in vivo and the effect of micromotion on bone ingrowth into a porous surface device under controlled loads in vivo [Abstract]. *Trans Orthop Res Soc.* 1991; 16: 103.
25. Friedman RJ, Black J, Galante JO, Jacobs JJ, Skinner HB. Current Concepts in Orthopaedic Biomaterials and Implant Fixation. *J Bone Joint Surg Am.* 1993; 75: 1086-1109.
26. Søballe K. Hydroxyapatite ceramic coating for bone implant fixation. Mechanical and histological studies in dogs. *Acta Orthop Scand.* 1993; 64: 1-58.
27. Søballe K, Hansen ES, Brockstedt-Rasmussen H, et al. Gap Healing Enhanced by Hydroxyapatite Coating in Dogs. *Clin Orthop Rel Res.* 1991; 272: 300-307.
28. Dalton JE, Cook SD, Thomas KA, Kay JF. The Effect of Operative Fit and Hydroxyapatite Coating on the Mechanical and Biological Response to Porous Implants. *J Bone Joint Surg Am.* 1995; 77: 97-110.
29. Ryd L, Albrektsson BEJ, Carlsson L, et al. Roentgen stereophotogrammetric analysis as a predictor of mechanical loosening of knee prostheses. *J Bone Joint Surg Br.* 1995; 77-B: 377-383.
30. Mjöberg B. The theory of early loosening of hip prostheses. *Orthopedics.* 1997; 20(12): 1169-1175.
31. Dhert WJA, Thomsen P, Blomgren AK, et al. Integration of press-fit implants in cortical bone: A study on interface kinetics. *J Biomed Mater Res.* 1998; 41: 574-583.
32. Åstrand J, Aspenberg P. Reduction of instability-induced bone resorption using bisphosphonates. High doses are needed in rats. *Acta Orthop Scand.* 2002; 73(1): 24-30.
33. Hilding M, Aspenberg P. Postoperative clodronate decreases prosthetic migration. 4-year follow-up of a randomized radiostereometric study of 50 total knee patients. *Acta Orthopaedica.* 2006; 77 (6): 912-916.
34. Drake MT, Clarke BT, Khosla S. Bisphosphonates: Mechanism of Action and Role in Clinical Practice. *Mayo Clin Proc.* 2008; 83(9): 1032-1045.

35. Russell RGG, Xia Z, Dunford JE, et al. Bisphosphonates. An Update on Mechanisms of Action and How These Relate to Clinical Efficacy. *Ann NY Acad Sci.* 2007; 209-257.
36. Black, DM, Delmas PD, Eastell R, et al. Once-Yearly Zoledronic Acid for Treatment of Postmenopausal Osteoporosis. *N Engl J Med.* 2007; 356(18): 1809-1822.
37. Lyles KW, Colón-Emeric CS, Magaziner JS, et al. Zoledronic Acid and Clinical Fractures and Mortality after Hip Fracture. *N Engl J Med.* 2007; 357: 1799-1809.
38. Arabmotlagh M, Rittmeister M, Hennigs T. Alendronate Prevents Femoral Periprosthetic Bone Loss Following Total Hip Arthroplasty: Prospective Randomized Double-Blind Study. *J Orthop Res.* 2006; 24: 1336-1341.
39. Venesmaa PK, Kröger HPJ, Miettinen HJA, Jurvelin JS, Suomalainen OT, Alhava EM. Alendronate Reduces Periprosthetic Bone Loss After Uncemented Primary Total Hip Arthroplasty: A Prospective Randomized Study. *J Bone Miner Res.* 2001; 16(11): 2126-2131.
40. Arabmotlagh M, Pilz M, Warzecha J, Rauschmann M. Changes of Femoral Periprosthetic Bone Mineral Density 6 Years after Treatment with Alendronate following Total Hip Arthroplasty. *J Orthop Res.* 2009; 27: 183-188.
41. Hilding M, Ryd L, Toksvig-Larsen S, Aspenberg P. Clodronate prevents prosthetic migration. A randomized radiostereometric study of 50 total knee patients. *Acta Orthop Scand.* 2000; 71(6): 553-557.
42. Wilkinson JM, Stockley I, Peel NFA, et al. Effect of Pamidronate in Preventing Local Bone Loss After Total Hip Arthroplasty: A Randomized, Double-Blind, Controlled Trial. *J Bone Miner Res.* 2001;16(3): 556-564.
43. Shetty N, Hamer AJ, Stockley I, Eastell R, Wilkinson JM. Clinical and radiological outcome of total hip replacement five years after pamidronate therapy: A trial extension. *J Bone Joint Surg Br.* 2006; 88-B(10):1309-1325.
44. Bobyn JD, Hacking SA, Krygier JJ, Harvey EJ, Little DG, Tanzer M. Zoledronic acid causes enhancement of bone growth into porous implants. *J Bone Joint Surg Am.* 2005; 87-B: 416-420.

45. Zometa. U.S. Food and Drug Administration website.  
[http://www.fda.gov/medwatch/SAFETY/2005/Oct\\_PI/Zometa\\_PI.pdf](http://www.fda.gov/medwatch/SAFETY/2005/Oct_PI/Zometa_PI.pdf).  
Accessed May 17, 2009.
46. Frost HM. A brief review for orthopedic surgeons: Fatigue damage (microdamage) in bone (its determinants and clinical implications). *J Orthop Sci.* 1998; 3: 272-281.
47. Mashiba T, Hirano T, Turner CH, Forwood MR, Johnston CC, Burr DB. Suppressed Bone Turnover by Bisphosphonates Increases Microdamage Accumulation and Reduces Some Biomechanical Properties in Dog Rib. *J Bone Miner Res.* 2000; 15(4): 613-620.
48. Mashiba T, Turner CH, Hirano T, Forwood MR, Johnston CC, Burr DB. Effects of Suppressed Bone Turnover by Bisphosphonates on Microdamage Accumulation and Biomechanical Properties in Clinically Relevant Skeletal Sites in Beagles. *Bone.* 2001; 28(5): 524-531.
49. Allen MR, Iwata K, Phipps R, Burr DB. Alterations in canine vertebral bone turnover, microdamage accumulation, and biomechanical properties following 1-year treatment with clinical treatment doses of risedronate or alendronate. *Bone.* 39: 872-879.
50. Chapurlat RD, Arlot M, Burt-Pichat B, et al. Microcrack Frequency and Bone Remodeling in Postmenopausal Osteoporotic Women on Long-Term Bisphosphonates: A Bone Biopsy Study. *J Bone Miner Res.* 2007; 22(10): 1502-1509.
51. Burr MD, Allen MR. Low Bone Turnover and Microdamage? How and Where to Assess It? [Letter]. *J Bone Miner Res.* 2008; 23(7): 1150-1151.
52. Amanat N, McDonald M, Godfrey C, Bilston L, Little D. Optimal Timing of a Single Dose of Zoledronic Acid to Increase Strength in Rat Fracture Repair. *J Bone Miner Res.* 2007; 22(6): 867-876.
53. Bobyn JD, Tanzer M, McKenzie K, Karabasz D, Krygier J. Locally Delivered Bisphosphonate for Enhancement of Bone Formation and Implant Fixation. Exhibit at the 2009 Annual Meeting of the American Academy of Orthopaedic Surgeons, Las Vegas, Nevada; February, 2009.
54. Goh SK, Yang KY, Koh JSB, et al. Subtrochanteric insufficiency fractures in patients on alendronate therapy: A caution. *J Bone Joint Surg (Br).* 2007; 89-B(3): 349-352.

55. Lenart BA, Lorch DG, Lane JM. Atypical Fractures of the Femoral Diaphysis in Postmenopausal Women Taking Alendronate. *N Engl J Med*. 2008; 358(12): 1304-1306.
56. Kwek EBK, Koh JSB, Howe TS, et al. More on Atypical Fractures of the Femoral Diaphysis [Letter]. *N Engl J Med*. 2008; 359(3): 316-318.
57. Lee P, Seibel MJ. Regarding letter, More on Atypical Fractures of the Femoral Diaphysis [Letter]. *N Engl J Med*. 2008; 359(3): 316-317.
58. Ezra A, Golomb G. Administration routes and delivery systems of bisphosphonates for the treatment of bone resorption. *Adv Drug Deliv Rev*. 2000; 42(3): 175-195.
59. Li EC, Davis LE. Zoledronic Acid: A New Parenteral Bisphosphonate. *Clin Ther*. 2003; 25(11): 2669-2708.
60. Garbuz DS, Hu Y, Kim W, et al. Enhanced Gap Filling and Osteoconduction Associated with Alendronate-Calcium Phosphate-Coated Porous Tantalum. *J Bone Joint Surg*. 2008; 90: 1090-1100.
61. Jakobsen T, Kold S, Bechtold JE, Elmengaard B, Søballe K. Local Alendronate Increases Fixation of Implants Inserted with Bone Compaction: 12-Week Canine Study. *J Orthop Res*. 2007; 25: 432-441.
62. Jakobsen T, Baas J, Kold S, et al. Local Bisphosphonate Treatment Increases Fixation of Hydroxyapatite-Coated Implants Inserted with Bone Compaction. *J Orthop Res*. 2009; 27: 189-194.
63. Tanzer M, Karabasz D, Krygier JJ, Cohen R, Bobyn JD. Bone Augmentation around and within Porous Implants by Local Bisphosphonate Elution. *Clin Orthop Relat Res*. 2005; 441: 30-39.
64. Gao Y, Zou S, Liu X, Bao C, Hu J. The effect of surface immobilized bisphosphonates on the fixation of hydroxyapatite-coated titanium implants in ovariectomized rats. *Biomaterials*. 2009; 30(9): 1790-1796.
65. Peter B, Gauthier O, Laib S, et al. Local delivery of bisphosphonate from coated orthopedic implants increases mechanical stability in osteoporotic rats. *J Biomed Mat Res Part A*. 2005; 76A(1): 133-143.
66. Peter B, Pioletti DP, Laib S, et al. Calcium phosphate drug delivery system: influence of local zoledronate release on bone implant osteointegration. *Bone*. 2005; 36: 52-60.

67. Stadelmann VA, Gauthier O, Terrier A, Bouler J-M, Pioletti DP. Implants delivering bisphosphonate locally increase periprosthetic bone density in an osteoporotic sheep model. A pilot study. *Eur Cell Mater*. 2008; 16: 10-16.
68. Roberts J. Studies on bisphosphonate elution from orthopaedic implants. Masters thesis, Department of Biomedical Engineering; McGill University; February 2008.
69. Paital SR, Dahotre NB. Calcium phosphate coatings for bio-implant applications: Materials, performance factors, and methodologies. *Mat Sci Eng R*. 2009; 66: 1-70.
70. Lindahl H, Malchau H, Herberts P, Garellick G. Periprosthetic Femoral Fractures: Classification and Demographics of 1049 Periprosthetic Femoral Fractures from the Swedish National Hip Arthroplasty Register. *J Arthrop*. 2005; 20(7): 857-865.